



Title	Study on Monitoring System for Forest Fires Based on Wireless Sensor Networks
Author(s)	Teguh, Rony
Citation	北海道大学. 博士(情報科学) 甲第11525号
Issue Date	2014-09-25
DOI	10.14943/doctoral.k11525
Doc URL	http://hdl.handle.net/2115/57288
Type	theses (doctoral)
File Information	Rony_Teguh.pdf



[Instructions for use](#)

Doctor Thesis

**Study on Monitoring System for Forest Fires
Based on Wireless Sensor Networks**

Rony Teguh

**A dissertation submitted in partial fulfillment
Of the requirements for the degree of
Doctor of Philosophy**

**Division of System Science and Informatics
Graduate School of Information Science and Technology
Hokkaido University**

Doctor Thesis
Submitted to Graduate School of Information Science and Technology
Hokkaido University
In partial fulfillment of the requirements for the degree of
Doctor of Philosophy

Rony Teguh

Thesis Committee:	Professor	Hajime IGARASHI
	Professor	Masahiko ONOSATO
	Professor	Hiroyuki KITA
	Associate Professor	So NOGUCHI

Study on Monitoring System for Forest Fires Based on Wireless Sensor Networks

Rony Teguh

Abstract

Indonesia has been suffered from forest fires. The recent fires in logger-over forest, peatland, and plantation should be classified into one of human-made disasters. In recent years, fires in Indonesia occurred mainly in peatland area and become one of international serious issues due to haze and CO² emission. One strategy to detection and monitor peat-forest fires in Central Kalimantan, Indonesia is to use a Wireless Sensor Networks (WSNs), which contains miniature sensor nodes to collect environmental data such as temperature, relative humidity, light and barometric pressure, and to transmit more accurate information to fire-fighter and remote monitor. In this study, in order to get real-time monitoring data of peat-forest fires, we develop the integration system of the WSN data used for the ground sensing with video surveillance data obtained from an unmanned aerial vehicle (UAV), which is used for ground verification of satellite data in large peat forest areas. In data processing of WSN in collaboration with UAV work, the most important issue is to allow quick responses in order to minimize the scale of the peat-forest fires.

We have an integration of system for the monitor of peat fires using wireless sensor network and the UAV, where a small fire is not detected by the satellite or in the dense smoke conditions. In-network processing data from WSN and UAV is the best strategy for monitoring peat-forest fire disasters. Monitoring wildfire system uses WSN containing the smart sensors to collect

environment data such as temperature, humidity, and barometric pressure, and to deliver useful information to fire-fighter or remote monitors. One way to verify the location of wildfire is to use UAV to collect more accurate information. The accuracy and reliability of combination data WSN and UAV are support largely impact to forest fire monitoring.

In forest, reliable communication in a dense or sparse environment is very important. Wireless sensor nodes must be able to effectively communicate data back to the base station. While battery power is limited and may not be rechargeable, wireless sensor nodes however can be equipped with a secondary power source such as solar cells. In any case, it is important for sensor nodes to save energy as much as possible. For monitoring and detect using WSN technology, energy can be conserved with multi-hop optimal routing, short transmission range, in-network data aggregation, eliminating data redundancy, minimizing delays, and using low duty-cycle. To maximize the lifetime of the energy-constrained WSNs, communication protocols such as LEACH and HEED have been developed in which the cluster heads are autonomously selected to share the energy loss in the sensor nodes. In this study, we develop optimization where the routers are optimally deployed to maximize the connectivity of the sensor nodes to the routers. The sensors are assumed to be randomly deployed to have wide coverage. We use genetic algorithm and simulated annealing for the optimization. We take the obstacles due to elevation differences into consideration in the optimization. Moreover, we consider the attenuation of electromagnetic waves in the forest. To evaluate the attenuation constant of the forest, we compute homogenized permittivity from the measured complex permittivity of tree trunks and basal area. It is shown that the horizontally polarized electromagnetic waves has smaller attenuation than the vertically polarized waves. We can know the necessary number of routers to have complete connections of sensors from the optimization results. Moreover, we can make optimal design of WSN topology for any vegetation and topography using the present method.

List of Contents

Abstract	i
List of Contents.....	iii
List of Figures	vi
List of Tables	viii
Chapter 1 Introduction.....	1
1.1 Background.....	1
1.2 Purposes.....	3
1.3 Thesis Outline.....	3
Chapter 2 Literature review.....	4
2.1 Peat forest fire monitoring.....	4
2.2 Wireless Sensor Network (WSN).....	5
2.3 Unmanned Aerial Vehicles (UAV).....	8
2.4 Originality of this study.....	10
Chapter 3 Forest fire monitoring system using remote sensing, UAV and WSN.....	11
3.1 Design WSN for forest fire monitoring	11
3.1.1 Sensor nodes	14
3.1.2 Base station	16
3.1.3 Sensor board.....	17
3.2 Deployment of WSN and UAV	18
3.3 Detection of potential fires	24
3.4 Verification of potential fires	27
3.5 Summary.....	29
Chapter 4 Propagation of EM waves in forest.....	30
4.1 Radio propagation in forest.....	30

4.1.1 Propagation modes in forest	31
4.1.2 Electromagnetic waves in absorbing media	32
4.1.3 Modeling of electromagnetic waves in forest	34
4.1.4 Homogenized permittivity of forest	36
4.2 Computation of attenuation constants.....	38
Chapter 5 Optimization of WSN in forest.....	41
5.1 Optimization method.....	41
5.1.1 Formation of wireless sensor networks	41
5.1.2 Wireless sensor networks deployment algorithm	41
5.1.3 Optimization using simulated annealing	42
5.2 Optimization results.....	43
5.2.1 Artificial test problem.....	43
5.2.2 Optimization of WSN for assumed attenuation constants	44
5.2.3 Optimization of WSN for computed attenuation constants	51
5.3 Summary.....	55
Chapter 6 Optimization of WSN in irregular terrain	56
6.1 Deployment of routers in elevation differences.....	56
6.2 Optimization problem.....	57
6.2.1 Problem definition	57
6.2.2 Real-Coded Genetic Algorithms (RGA).....	59
6.3 Optimization results.....	60
6.3.1 Optimization of WSN with small communication radius.....	61
6.3.2 Optimization of WSN with large communication radius	63
6.3.3 Number of disconnected sensors	65
6.4 Summary.....	67

List of Contents

Chapter 7 Conclusions.....68

References

Acknowledgement

List of Figures

Figure 1.1: Map of peatland distribution in the Southeast Asia [1].....	1
Figure 2.1: The system architecture monitoring peat forest fires	5
Figure 2.2: The Cluster networks topology.....	7
Figure 2.3: The Layered communication.....	8
Figure 2.4: An illustration of UAV observation in peat forest fires.....	9
Figure 3.1: Flowchart for detection and verification of potential peat forest fires.....	11
Figure 3.2: IRIS mote [84]	16
Figure 3.3: Stargate Netbridge and MIB520 [84]	17
Figure 3.4: MTS400 module [84]	18
Figure 3.5: Location of tropical rain forest site in Kalimantan	18
Figure 3.6: Sensor network deployed at peat forest.....	19
Figure 3.7: The n^{th} Fresnel zone [56]	21
Figure 3.8: UAVs mission of observation area [7].....	23
Figure 3.9: Flow of information fire WSN data.....	25
Figure 3.10: Temperature data detection of fire.....	26
Figure 3.11: Humidity data detection of fire.....	27
Figure 3.12: Comparison of data WSN with UAV photo	28
Figure 4.1: Radio wave propagation in the forest.....	32
Figure 4.2: Sensing field in tropical peat forest in Central Kalimantan, Borneo	34
Figure 4.3: Communication distance R in lossy sensing field.....	39
Figure 4.4: Number of routers N for full coverage of sensing field of 10^6 m^2	
R_0 [m] represents communication distance in free space	39
Figure 4.5: Attenuation constants in P2 for different polarization.....	40

List of Figures

Figure 5.1: Artificial problem with attenuation area with $\alpha=1/100$ near base station, $RN=12$	43
Figure 5.2: Location of tropical rain forest site in Central Kalimantan, Borneo.....	44
Figure 5.3 Sensing field in grassland and forest	45
Figure 5.4: Optimized results for $RN=5$	47
Figure 5.5: Optimization histories for $RN=5$	47
Figure 5.6: Optimized topology for inhomogeneous $RN=12$	49
Figure 5.7: Optimization histories for $RN=12$	49
Figure 5.8: Number of connected sensors.....	50
Figure 5.9: Optimization results for uniform sensing field, BS, RN, SN represent base station, router and sensor nodes, NR is number of routers $\alpha= 3 \times 10^{-3}$, $R_o=500m$	53
Figure 5.10: Optimization results for sensing field shown in Fig.4.2 $R_o=750m$	54
Figure 6.1: WSN in irregular terrain. The color represents elevation	57
Figure 6.2: Test communicability of the sensor nodes.....	59
Figure 6.3: Optimized topology for flat terrain, $R_s=R_r=100m$, $M=5$	61
Figure 6.4: Optimized topology for irregular terrain, $R_s=R_r=100m$, $M=5$	62
Figure 6.5: Optimization history when $R_s=R_r=100m$, $M=5$	62
Figure 6.6 Optimized topology for flat terrain, $R_s=R_r=400m$, $M=5$	63
Figure 6.7: Optimized topology for irregular terrain, $R_s=R_r=400m$, $M=5$	64
Figure 6.8: Optimization history when $R_s=R_r=400m$, $M=5$	64
Figure 6.9: Number of disconnected sensor nodes for optimized WSN in flat terrain	65
Figure 6.10 Number of disconnected sensor nodes for optimized WSN in irregular terrain.....	66
Figure 6.11: Number of disconnected sensor nodes for non-optimized WSN in flat terrain.....	66
Figure 6.12: Number of disconnected sensor nodes for non-optimized WSN in irregular terrain	67

List of Tables

Table 3.1: The hardware information about IRIS mote	15
Table 6.1: Simulation parameter	60
Table 6.2: RGA parameter setting	60

Chapter 1 Introduction

1.1 Background

Recently large-scale tropical peat forest fires have frequently taken place in boreal and tropical rain forests. They can give significant impacts on environment and human society. In particular, peat and forest fires in Indonesia are said to be one of the dominant causes of the global warming. In fact, the peat and forest fires in central Kalimantan and Borneo released between 0.8 and 2.57 Gt of carbon which is equivalent to 13-40% of the mean annual global carbon emissions from fossil fuel in 1997 (see Fig.1.1)[1]. In Central Kalimantan, Indonesia, peat forest fires are mostly anthropogenic. Fires are used by local and immigrant farmers as part of small farmland activities such as land clearance[2]. During droughts, some fires spread out of control and become wildfire in peat forest areas. Fires in peat forest land not only burn the surface vegetation, but also the peat deposit up to 100 cm below the surface. However, peat fires occur only in extreme drought conditions or after the ground water level is lowered artificially[3].

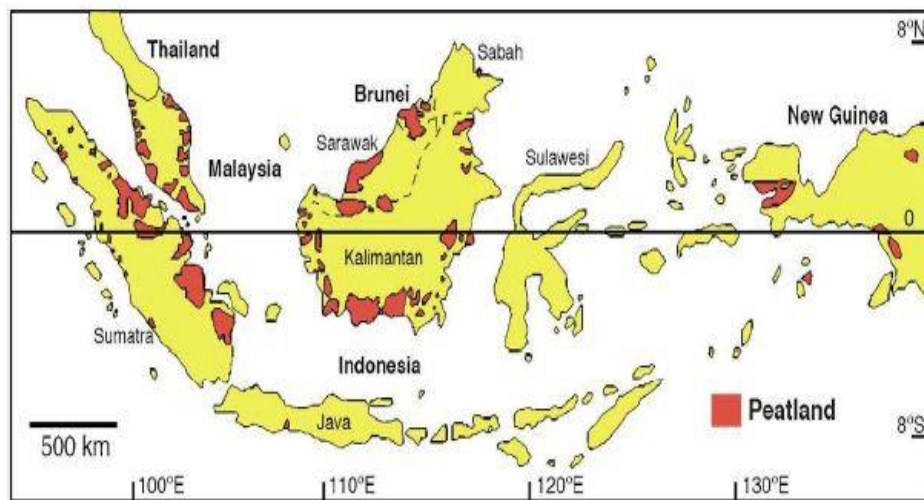


Figure 1.1: Map of peatland distribution in the Southeast Asia [1].

Peat fires produce large amount of smoke and deteriorate air quality; the dense haze also causes various health problems. For long time the peat fires have had negative impacts on economy, human health, environment, and climate[4]. Wildfires caused by lighting, spontaneous combustion, human activities and so on are serious problems especially in North America, Siberia and Indonesia. Wildfire can give rise to significant health, economic and environmental damages. Identification of potential peat-forest fires and fire zones has been done by remote sensing[5].

In Kalimantan and Sumatra, a few ten thousand wildfire events were detected a year by MODIS[6]. Problem found in monitoring of fires in peat lands by satellites is that small or weak fires cannot be detected. Fires in peat land burn not only the surface, but also the underground. Weather conditions have significant influences on fire behavior. The dry season in Central Kalimantan lasts normally for two months per year, July and August, while abnormally dry season lasts for 4-5 months. Tropical peat is usually formed from woods, whereas boreal peat is composed of sphagnum and grasses. Due to their higher calorific values, tropical peat materials are more flammable than other fuels, especially when they are dry.

One of the most promising detection systems is that based on wireless sensor networks (WSN) and unmanned aerial vehicle (UAV). In the WSN detection, many sensors are deployed in the target area to measure environmental data such as temperature, humidity and light. The measured data are then aggregated to the base station (BS) through wireless communication. This system can realize fast and direct detection of wildfire. Because initial detection of wildfire is important for effective extinction, a detection system using UAV and WSN for Indonesian wildfire has been developed [7]. The integration system of the WSN data is used for the ground sensing with video surveillance data obtained from an unmanned aerial vehicle (UAV), which is used for ground verification of satellite data in large peat forest areas. The combination of WSN and UAV promises early detection of peat forest fires in Indonesia. WSNs have several functions such as sensing, data processing and communication, and work as a platform for processing of distributed data collected from wide environment. The sensors in WSNs operate with limited

power and wireless communication capability. Especially, energy usage is significant concern in WSNs placed in wild environment since it is difficult to make frequent replacement of batteries in the sensors. Transmission range is important aspect on the placement of sensor network. Increase of coverage requirement enhances the accuracy of the sensed data.

1.2 Purposes

The purposes of this study are:

1. Integration of the system for detect peat fires using WSN and UAV, it is useful for help fire patrol to fire findings and measurement of fire size, counting of fires.
2. Optimization of router deployment effective operation of WSNs in forest, vegetation and elevation to maximize the lifetime of the energy-constrained WSNs. In the optimization, we take the attenuation of electromagnetic wave in the forest and geometries of the sensing field into account.

1.3 Thesis Outline

This thesis is organized as follows:

In Chapter 2, discussed literature review studied monitoring system on tropical peat forest fire with wireless sensor network and Unmanned Aerial Vehicle (UAV). Chapter 3, the author will make detailed discussion of the Wireless Sensor Network (WSN) and Unmanned Aerial Vehicles (UAV) for detection and verification potential peat forest fires. Chapter 4, the author will make discusses propagation electromagnetic in forest. Chapter 5 gives the optimization model used and clustering techniques of WSN. It further presents the Zigbee protocol system and explains the impact of forest and elevation in WSN with an in-depth discussion of the experiments performed. Chapter 6 gives the optimization model wireless sensor network in flat and irregular terrain. Chapter 7 concludes the thesis and presents the future direction and implication for WSN.

Chapter 2 Literature review

2.1 Peat forest fire monitoring

Fig. 2.1 shows the concept design of WSN and UAV for ground monitoring system in Central Kalimantan, Indonesia. System architecture has 3 layers. Sensor network layer provides ground-sensing environment. Unmanned aerial vehicle (UAV) layer performs low altitude video surveillance, and satellite layer provides monitor of the earth surface in different spectral bands of the visible, infrared and radar frequencies. The accuracy and reliability of satellite-based systems are largely influenced by weather conditions. Traditionally, the fire monitoring task was performed by human observations. However, the reliability of this method is in doubt. Satellite imaging can be used to detect large areas, where the minimum detectable fire size is 0.1 hectare, and the fire location accuracy is 1 km. For fire detection, complete images of land are collected every 1 to 2 days. For this reason, the systems cannot provide timely detection. To get real-time monitoring data of peat-forest fires, we employ WSN for the ground sensing with aid of video surveillance performed by an unmanned aerial vehicle (UAV). This system can also be used for ground verification of satellite data in large peat forest areas. In data processing of WSN in collaboration with UAV, the most important issue is to allow quick responses in order to minimize the scale of the peat-forest fires. The sensor nodes can relay the exact origin of the fire to the end users before the fire spreads to be uncontrolled. The system is useful for fire patrol to find fire and to measure of fire size, and to count fires.

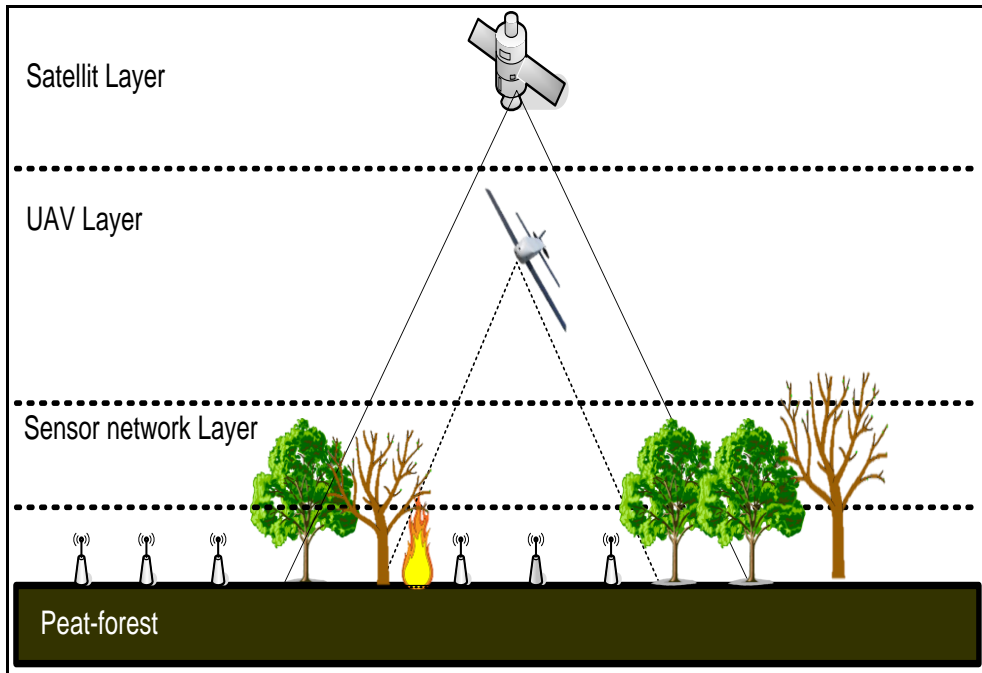


Figure 2.1: The system architecture monitoring peat forest fires

To realize an effective system shown in Figure 2.1, optimal deployment strategy for sensor and router nodes must be carried out considering cost, as well as sensing radius and sensing accuracy of environment parameters. An important aspect of network reliability is the transmission range. In case of long range transmission in forest obstructions which are caused by tree and vegetation may reduce the transmission range. Distance estimation is the key factor of wave signal propagation for optimal placement of sensor [8], [9], [10]. Appropriate transmission power is essential for all nodes to have appropriate connectivity.

2.2 Wireless Sensor Network (WSN)

WSNs have great potential for many applications in scenarios such as military target tracking and surveillance[11][12], hydrology[13], forest fires monitoring [7][14][15][16], farming monitoring[17][18][19], healthcare monitoring[20][21], natural disaster[22][23][24], and hazardous environment exploration and seismic sensing[25]. Recently, researchers have proposed the use of some special nodes, called relay nodes [26] [8][27], within the network, for balanced data gathering, to achieve fault tolerance and to extend network lifetime. The relay nodes can be

used as cluster-heads/router in hierarchical sensor networks[28][29][30], and can be provisioned with higher energy[31][32][33], as compared to the sensor nodes.

The large-scale deployment of wireless sensor networks (WSNs) and the need for data aggregation necessitates efficient organization of the network topology which realizes load balancing and prolongation of the network lifetime[34][35][36]. Clustering has proven to be an effective approach for organizing the network. Clustering techniques in wireless sensor networks aim at gathering data among groups of nodes, which elect leaders among themselves[28][30][29]. The cluster-heads or routers aggregate the data and transfer the aggregated data to the base station (BS). The advantage of this scheme is the reduction of energy usage of each node and communication cost. In order to support data aggregation through efficient network organization, nodes are partitioned into a number of small groups called clusters.

Each cluster has a coordinator, referred to as a cluster head/router, and a number of member nodes. Clustering results in a two-tier hierarchy in which cluster heads (CHs) form the higher tier while member nodes form the lower tier[37][38][39][40]. Figure 2.2 illustrates data flow in a clustered network. WSNs consist of sensors, routers and a base-station, which work together to collect data about the status of the target field. The sensors perform periodic measurement of environmental data such as temperature and humidity and send them to the routers or directly to the base station node. The routers collect data from the sensor nodes to send them to the base station. WSNs have several functions such as sensing, data processing and communication, and work as a platform for processing of distributed data collected from wide environment[32], [41].

In WSNs based on the Zigbee system[42][43], measured data are sent by UHF-band electromagnetic waves from sensor nodes to routers or directly to the base station. The routers gather measured data and send them to the base station via multihop communication. One of the largest problems in operation of WSNs is that they have energy constraints: the sensor and router nodes usually have limited energy source such as batteries[44][45] and solar panels[46][47]. It is impractical to make frequent replacement of the batteries in the sensor nodes

widely deployed in forests. Moreover, sufficient energies for proper operation of the sensor nodes cannot be provided from the batteries charged by the solar panels due to bad weather conditions.

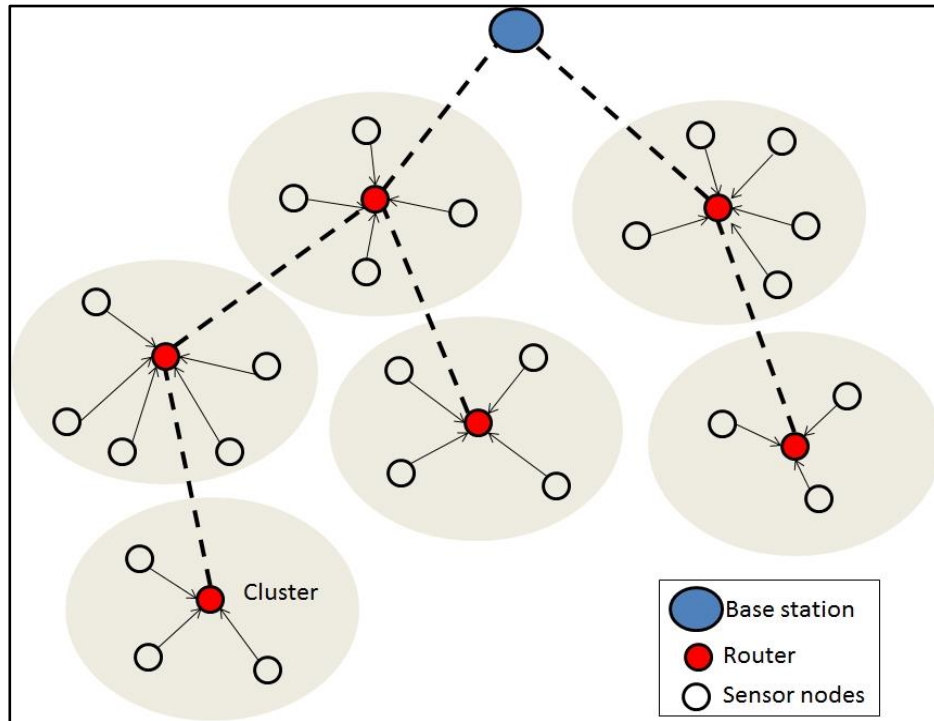


Figure 2.2: The Cluster networks topology

To maximize the lifetime of the energy-constrained WSNs, communication protocols such as LEACH [28] and HEED [30] have been developed in which the cluster heads are autonomously selected to share the energy loss in the sensor nodes. The cluster head collects data from the sensors in its cluster to send them to the base station. On the other hand, the routers which play a similar role as the cluster heads are predicate in Zigbee systems, which we will consider in this study.

A layered communication is performed among a base station and sensors scattered in the field. The sensor nodes near the base station constitute a single hop count to the base station, while nodes that are farther away constitute multiple hop count to the base station depending on the size of the network, this is shown in Figure 2.3. The goal of layered communication design is to support multi-hop routing. The packets are forwarded to nodes closer to the BS and produce more residual energy. A simplified routing scheme unlike in ad hoc networks has been proposed

in[48]. The goal is to achieve a more power efficient protocol. Recently, other protocols [49][29] specifically designed to accommodate routing and packet forwarding have been proposed.

In the wild environment, sensor nodes will collaborate with each other to perform distributed sensing and overcome obstacles, such as trees and rocks that block wired sensors line of sight. Since the WSNs for wildfire monitoring are usually deployed in area that is difficult to access, the power source has to support the long-term operation of a sensor node. The sensor node operates on limited battery power. When it dies and disconnects from the network, the performance of the application is significantly affected. The sensors can take turns to sleep and work to create a balance in the energy consumption in order to maximize the WSN lifetime.

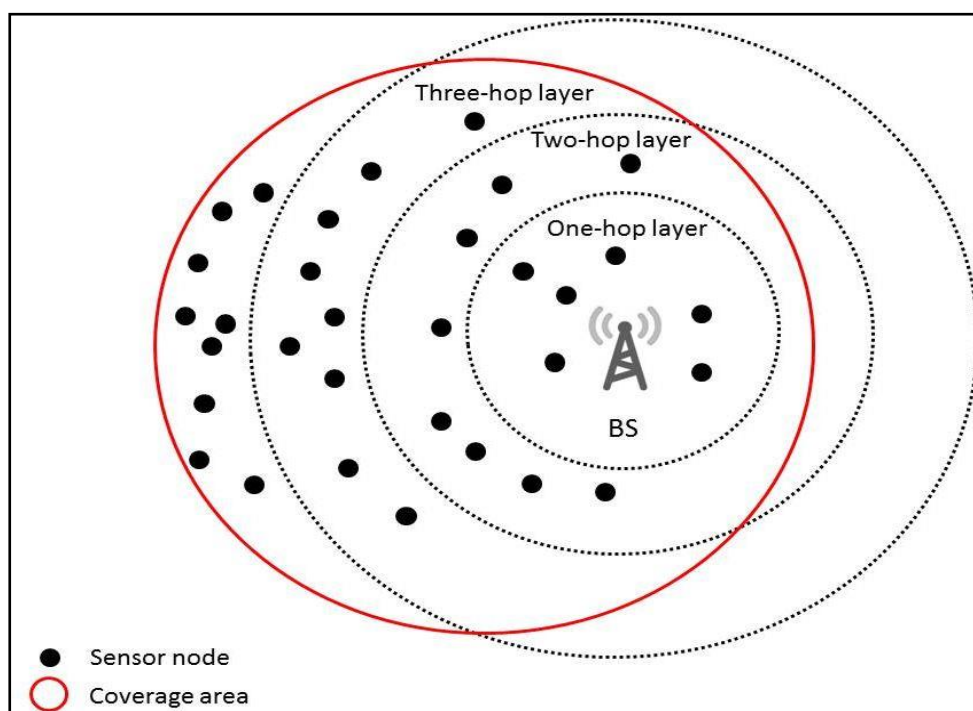


Figure 2.3: The Layered communication

2.3 Unmanned Aerial Vehicles (UAV)

For early wildfire detection there are vertical and horizontal technique. The horizontal technique is using surveillance of tower with human vision and video based monitoring[50] and vertical technique includes remote sensing. For remote sensing we can use satellite, unmanned aerial vehicles (UAV) or aircraft. These methods are based on the pictures taken by the satellite or

UAV, which enable us to monitor any potential fire. UAVs have been already deployed after several disasters[51] [52], and installed camera was used to assess the situations. UAV flying up to 100 meters high takes pictures for ground information. In the case of wildfire verification and fire detection, it is important to have an accurate and up-to-date overview of situation. The UAV is useful for this purpose because it can fly to the target place to verify the environmental conditions.

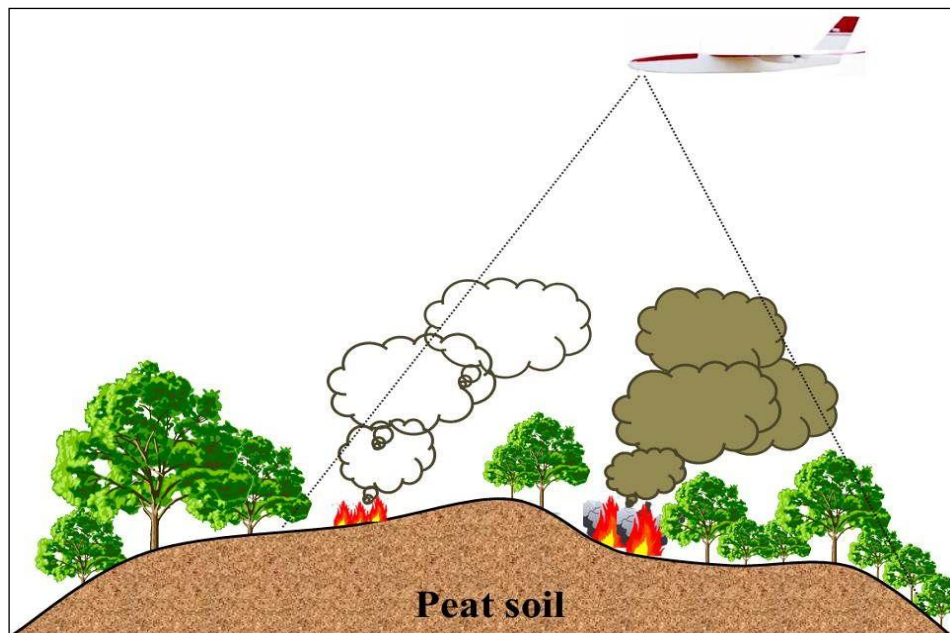


Figure 2.4: An illustration of UAV observation in peat forest fires

Figure 2.4 shows a UAV route to visit all picture taking-points. This enables the planning of observation area, execution of mission and analysis of the video surveillance by UAV. During the UAV flight, we can use infrared video and color camera to extract information of the covered area. The resulting image data from the UAV will be compared with the data from satellite or WSN to identify the fire hazard area more accurately. Collecting real-time data from WSN and UAV would be the best strategy for monitoring peat-forest fire disasters. The wildfire monitoring system uses WSN which consists of the smart sensors to collect environment data such as temperature, humidity, and barometric pressure, and to deliver useful information to fire-patrols or remote monitors.

2.4 Originality of this study

The author claims the originality of the present study against the above mentioned previous works in the following points:

1. The new wildfire detection system is proposed. In this system, when the abnormal temperature is detected by a sensor node in the WSN, UAV flies near to the sensor to take picture of the forest. If fires are observed in the picture, fire patrol is called immediately. This two-step procedure has not been proposed by other researchers as far as the author knows.
2. In this study, the sensors are assumed to be placed randomly to cover the target field. On the other hand, the router positions are optimized to maximize the connectivity of the sensor nodes. This optimization problem has not been discussed by other researchers. Moreover, in this study, the author takes the attenuation of electromagnetic waves by the tree trunks and scattering due to irregular terrain into account. These points have not been considered in the previous optimization of WSNs.

Chapter 3 Forest fire monitoring system using remote sensing, UAV and WSN

3.1 Design WSN for forest fire monitoring

One way to monitor peat-forest fires in Central Kalimantan, Indonesia, is to use a wireless sensor network (WSN), which contains miniature sensor nodes to collect environmental data such as temperature, relative humidity, light and barometric pressure, and to transmit more accurate information to fire patrol and remote monitor. Recently, considerable advances have been made in hardware and software technologies for building wireless sensor networks. Figure 3.1 shows the proposed approach of forest fires detection based on WSN.

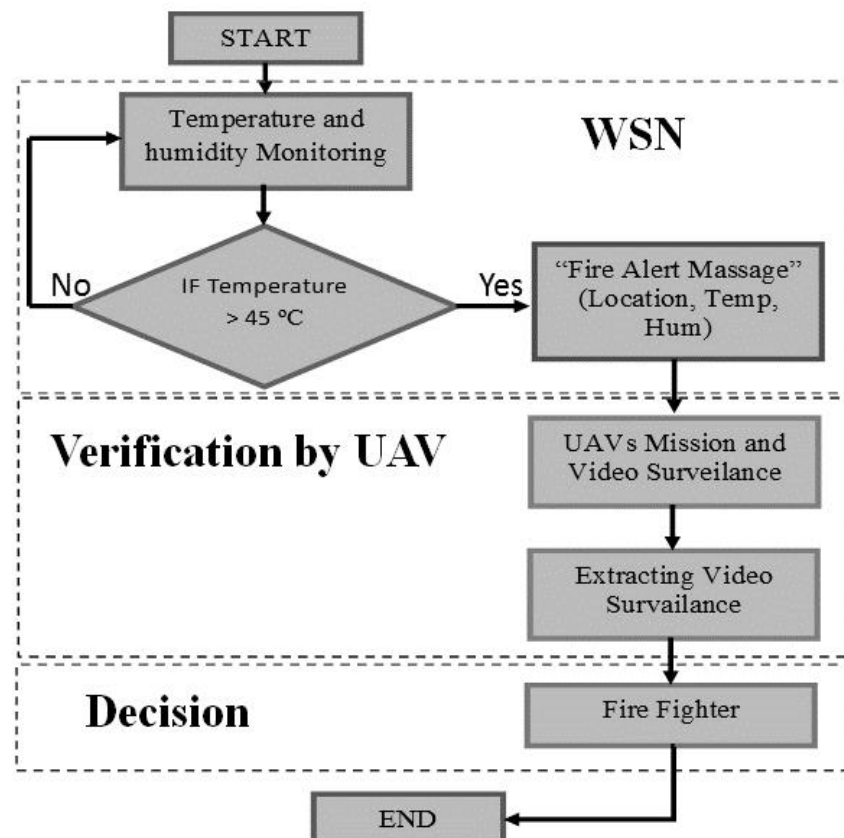


Figure 3.1: Flowchart for detection and verification of potential peat forest fires

In Fig.3.1, our proposed approach of forest fires detection based on WSN and UAV. The process is start for detection and monitoring forest fire. The sensor nodes period monitor of fire temperature and humidity data in forest environment. If sensor nodes detect of the temperature higher than 45°C is considered to be caused by potential fire. The sensor nodes directly send information GPS location, temperature and humidity to base station/remote monitor by multihop communication. To verification, the UAV perform video surveillance and can take the images by the infra-red and visible ray cameras. Finally, data collaboration from WSN and UAV can help find fire and measure of fire size to quick response for fire fighters minimize the scale of fire.

In this study, in order to get real-time monitoring data of peat-forest fires, we have developed integration system of the WSN data used for the ground sensing with video surveillance data obtained from an unmanned aerial vehicle (UAV), which is used for ground verification of satellite data in large peat forest areas. In data processing of WSN in collaboration with UAV, the most important issue is to allow quick responses in order to minimize the scale of the peat-forest fires. The developed system for detect peat fires using WSN and UAV is expected to help fire patrol to find fire and measure of fire size. In this section, we describe our WSN-based fire detection system. In the following, the author lists the important design goals and features that a wireless sensor network should have in order to be able to successfully monitor forest fires [41].

1. **Energy efficiency:** Sensor nodes are powered with batteries; therefore a wireless sensor network deployed for fire detection should consume energy very efficiently. Energy consumption should also be balanced fairly among nodes. Usually the deployment area is very large and thousands of sensor nodes may be needed, and therefore replacing batteries may be too costly, impractical or even not possible.
2. **Early Detection and Accurate Localization:** It is important to detect a forest fire as early as possible and to estimate the fire location at high accuracy. A forest fire usually grows exponentially and it is crucial that the fire should be detected and interfered in about six minutes to prevent the fire from spreading to a large area. Accurate estimation of the fire

position is important to send the firefighting personnel to the correct spot in the shortest possible amount of time.

3. **Forecast Capability:** It is important to forecast the spread direction and speed for planning firefighting. It is also important to be proactive in mobilizing resources, and to warn the surrounding area. Accurate forecasting requires accurate and fresh sensory data which arrive at the decision and control center from all points of the forest, especially from and around the region where the fire has occurred (i.e., critical zones).
4. **Adapting to Harsh Environments:** A sensor network for forest fire detection will operate usually in harsh environments and therefore should be able to deal with and adapt to harsh conditions. It should be able to recover from node damages, link errors, high temperature, humidity, pressure, etc.

Figure 2.1 shows the concept design of WSN and UAV for ground monitoring system in Central Kalimantan, Indonesia. System architecture has three layers. Sensor network layer provides ground-sensing environment. Unmanned aerial vehicle (UAV) layer provides monitor of low altitude video surveillance, and satellite layer provides monitor the earth surface in different spectral bands of the visible, infrared and radar frequencies.

The methodology of the forest fire monitoring includes the following three major modules for data collection, communications through the network and analysis of collected data.

- **Data collection module:** This module makes it possible to capture the various weather conditions necessary for the calculation of index (or formulas). This runs periodically until an event of detection of fire takes place.
- **Communication module:** It is used to route urgent data (alarms) generated by the data collection module to the analysis module within certain parameters of quality of service (QoS) such as reliability (the alarm must arrive at sink safely), temporal constraint (alarm must arrive within a reasonable time) and security (the routing path taken by the alarm must be secure against any attack or malicious behavior).

- **Analysis module:** After receiving the data in accordance with application of parameters of required QoS, the analysis module must examine the received alarms. Then, this information is processed by the decision-making center that can judge if it is a false alarm by either using the data collected from other sensors nodes or dispatching a team to check the situation locally.

3.1.1 Sensor nodes

Sensors are deployed in a forest before the fire may occur. Due to the non-homogeneity of the forest vegetation, it is almost impossible to deploy the sensors in forest at regular grid points. The system should be able to perform well even in a random distribution of sensors. The main function of the sensors is to locate the fire. This can be achieved with many sensor types, such as light or temperature sensors, or even cameras. Because the sensors located very close to the fire (below the burning range) are burning, they cannot send any data. When the sensors that are at outside of the sensitivity range from the fire report ambient temperature, their data are useless.

Thus, each sensor can only accurately determine the distance to the closest fire, if it is sufficiently away from the burning range and sufficiently close to the sensitivity range. The temperature readings together with sensor geographical coordinates are sent hop by hop through other sensors to one of the base stations. Because the sensors should know their own positions, they have to be programmed during the deployment process. Wireless sensor networks are also commonly considered as a means that is able to monitor an endangered forest area and detect fire. The basic data gathered by simple wireless sensors, that is, temperature, humidity and air pressure readings, can be used to determine the presence of fire.

The sensor node that we have adopted is the Crossbow IRIS mote[84]. This is the most recent version of the Mica mote, which has been employed in a number of practical WSNs. The MEMSIC Crossbow IRIS mote is operated using TinyOS[53][54], which is specifically developed for programming small devices with embedded microcontroller.

The main functions of the sensor nodes are communication, data processing, and sensor. In addition, TinyOS is programmed largely in the NesC, which supports a component-based, and event-driven programming to build applications in the TinyOS platform. Collecting real-time data from WSN is important for understanding of the state of peat and forest environment and allows predictive analysis of fire extension. The sensor nodes include communication and sensor board module. Communication module of IRIS mote uses the IEEE 802.15.4 protocol [55][42], which has a 250kbps data-rate. Transmission range is 500m-outdoors light of sight and 100m indoors when using a 1/4-wave dipole antenna and RF power 3 dBm. The characteristics of this sensor node are summarized in Table 3.1.

Table 3.1: Characteristics of the IRIS mote

Component	Description
Processor	Atmel AT Mega 128L
Program flash memory	128K byte
Configuration EEPROM (data)	4K byte
Frequency	2400-2480Mhz
Radio transceiver	CC2430
RF Power	3dBm
Receiver sensitivity	-101 dBm
Outdoor range	500m
Indoor range	100m
Battery	2 AA batteries

One of the most important constraints on sensor nodes is the low power consumption requirement. Sensor nodes carry limited, generally irreplaceable power sources. Therefore, while traditional networks aim to achieve high quality of service (QoS) provisions, sensor network protocols must focus primarily on power conservation.

Fig 3.2 represents the test-bed used in this study. It includes four battery powered motes IRIS and one gateway MIB520. Each mote is an assembly of MTS400 sensor-board (see Fig.3.4) and MPR2600 board which contains mainly a microcontroller, memory and communication module with Zigbee model at 2.4 Ghz ISM band.



Figure 3.2: IRIS mote [84]

3.1.2 Base station

In the forest, there are also a certain number of base stations. These are able to communicate freely with each other. Their processing abilities are also much higher than in the case of the sensors. Base stations gather the temperature readings delivered by the sensors. One of the base stations acts as a network center and merges all the data together. Sensors can send data to other sensors and/or base stations only if they are connected with a base station either directly or by multiple hops. During a forest fire, the network topology is reduced, step by step. Some nodes are burned or destroyed, and some of them lose their connection with the base stations when their neighbors are destroyed by fire. As the sensors should know their positions, geographical routing and MAC protocols are suitable in order to deliver the data to the base stations.

The base station consists of XM2110CA, communication module, which is the same as that used by the IRIS mote, and a Stargate Netbridge (see Fig. 3.3). This operates a SQLite database server and a web server, and can be connected to internet by wired ethernet. The database server stores acquired data, and makes it available through the web server. It can also send emergency messages to clients if an extreme temperature or humidity is detected. Fire alarm may receive by

smart phone. The gateway manager node provides types of information for users to generate emergence report for abnormal event when extremely high temperature is detected.



Figure 3.3: Stargate Netbridge and MIB520 [84]

3.1.3 Sensor board

Each onboard sensor measures different data such as temperature, light, acceleration, humidity, and pressure (see Fig. 3.4). The mote can be configured to capture, process and communicating by radio simultaneously. The gateway MIB520 is connected through USB cable to user computer to serve as programming interfaces of IRIS platforms. All motes communicate with each other wirelessly.

The sensor board module is responsible for data analog digital conversion and collecting parameters such as relative humidity of the atmosphere and air temperature. The processing module is responsible for controlling the operation of the whole sensor node and saving and coping with data collected by its own node and the binary information transmitted from other nodes. The wireless communication module is responsible for communication with other nodes and exchanging control information and receiving or transmitting data. The power module supplies power for the other three modules and drives the nodes, making it the key factor for the effective operation of the network.



Figure 3.4: MTS400 module [84]

3.2 Deployment of WSN and UAV

For experiment and implementation, WSN and UAV have been deployed to detect and monitor the peat forest in Central Kalimantan, Indonesia[7]. The map of the location is obtained from Landsat images (see Fig. 3.5). There are forest, grassland and free space. In this study we use the System for automated Geoscientific Analyses (SAGA)[85] to extract the information about forest and vegetation from Landsat images.

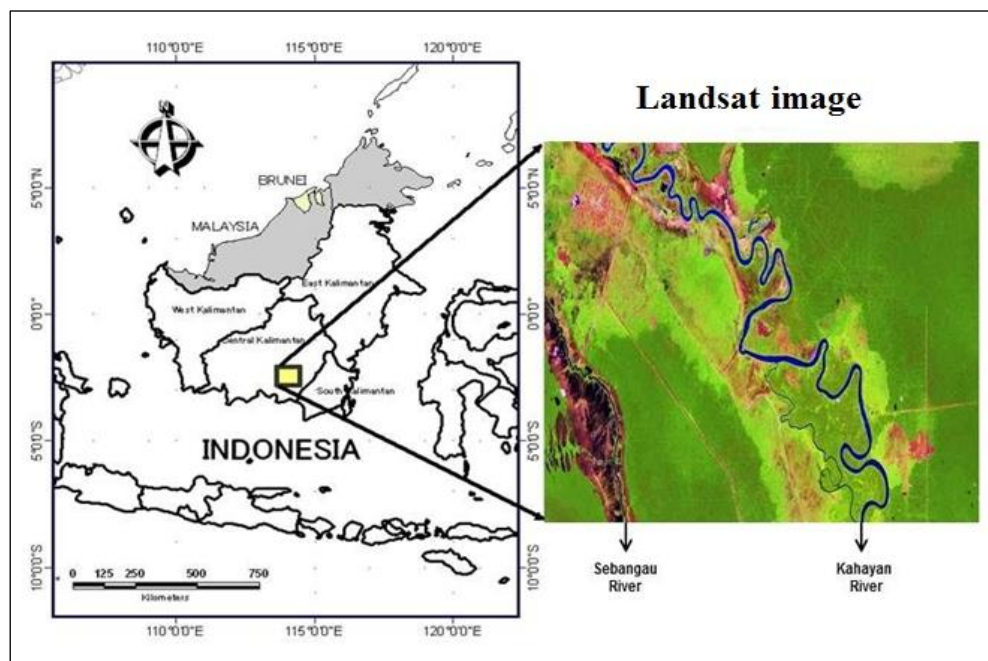


Figure 3.5: Location of tropical rain forest site in Kalimantan

Figure 3.6 shows that the WSN includes 6 sensor nodes, gateway terminal and MoteView[88] applications for monitoring. The distance between each sensor node is 100 meters, and the height of sensor nodes from ground is 1.5 meters. This system can detect a small fire of about three meters in size. In this work, sensor nodes are deployed in peat forest environment, where the height of vegetation in the peat forest area ranges from 1 to 5 meters from the ground, which will affect WSN signal strength and radio propagation.

Transmission range is important aspect in the placement of sensor network. Increase of coverage requirement enhances the accuracy of the sensed data. The deployment technique of sparsely sensor deployment may result in long-range transmission and high-energy usage while densely sensor deployment may lead to short-range transmission and less energy consumption. The network topology must be designed so that energy can be saved while it provides optimal multi-hop routing for efficient and reliable data delivery and link quality.

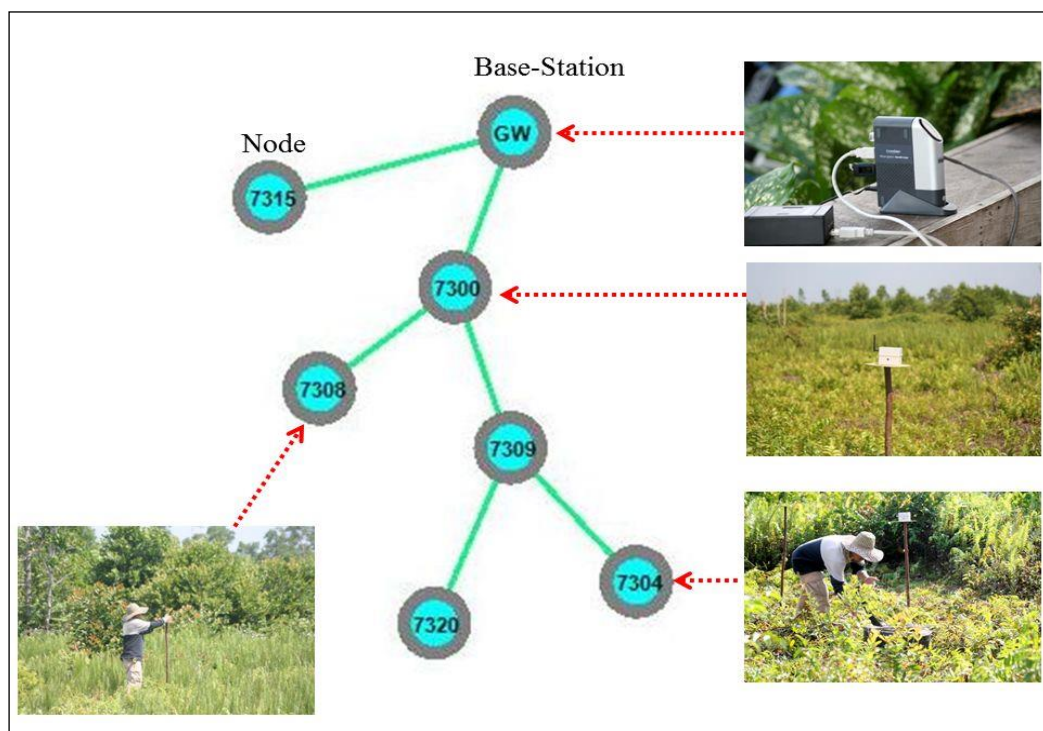


Figure 3.6: Sensor network deployed at peat forest

Sensing coverage and network connectivity are very important for sparsely deployment; efficient node deployment strategies in wide area would minimize cost, and reduce computation and communication. Fig. 3.6 shows sensor node network installation by manual deployment of sensor node positions at peat forest. In the experiment of the field sensor network, we take the two factors into consideration: (1) the quality of environment sensing, and (2) the amount of energy consumption. For the quality of sensing, we focus on the coverage of sensing of environment parameter. Simultaneously, we have to consider the energy consumption to lengthen the lifetime of the WSN. The multi-hop communication is exploited to relay sensed data from sensor nodes to base station. Hence nodes to base station have a priorities data packet communication load and thus consume more energy. One of the channel, ranging from 1 to 12, is automatically given for the sensor communication. The quality of wireless signal highly depends on the application, environments characteristics and frequency spectrum used. Typical propagation environment consist of tree and vegetation, which act as obstacles in the radio communication and cause scattering and absorption. The radio propagation in wireless communications experiences signal-strength loss due to distance, frequency, antenna gain and power.

The key factors that affect the signal in WSN are height from ground, signal distance, ground reflection, vegetation obstruction and diffraction, and antenna radiation pattern. Free space loss is widely used for an ideal propagation condition with no obstacles nearby to cause reflection or diffraction. It is possible to predict the signal strength at the receiving node when there is a clear line of sight (LOS) path between the transmitting and receiving nodes. The received signal power decreases with increasing distance between the transceivers. However, for obstructed paths, it is not adequate just to use free space loss model to predict the signal strength when the radio is near the ground. The antenna height and vegetation density are important parameters that affect communication networks coverage and connectivity. To maximize the connectivity, the antenna height must clear the Fresnel zone.

Another problem that we encountered was the reduction of transmission range by

obstructions in the Fresnel zone. Since obstructions can produce reflected signals that will be out of phase with the main signal, it is important that an adequate size of Fresnel zone is kept clear in order to maximize the transmission range and the hence success rate.

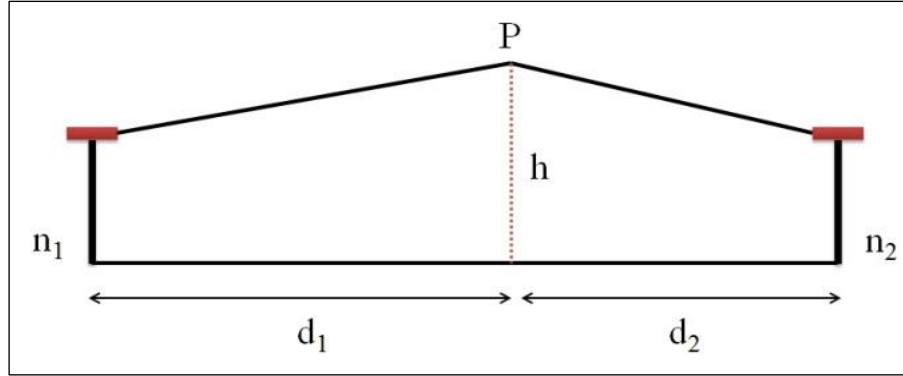


Figure 3.7: The n^{th} Fresnel zone [56]

Fig. 3.7 shows the n^{th} Fresnel zone between two nodes, n_1 and n_2 . In early implementation, nodes were placed only on the ground, but we found that this arrangement drastically reduced the transmission range because of the small Fresnel zone. The radius of a n^{th} Fresnel zone is calculated as follows [56]:

$$R_n = \sqrt{\frac{n\lambda d_1 d_2}{d_1 + d_2}} \quad (3.1)$$

In this equation, R_n is the radius of the cross-section of the n^{th} Fresnel zone at the arbitrary point P , λ is the wavelength, and d_1 and d_2 respectively are the distance to the sender and receiver from the point P . For wireless radio communication at $f=2.45\text{GHz}$, the maximum Fresnel zone radius is about 1.75 and 1.25 m when $d_1=d_2=50$ and 25m, respectively. Therefore, nodes ought to be at least 1.25m above the ground in order to eliminate interference when the communication distance is 50m. Thus, although the specification of the IRIS mote suggests that the transmission range is more than 300m outdoors, we found it difficult for nodes 50m apart to communicate each other. If nodes were deployed densely, this problem might not be significant, which is not the case for a sparse network like ours.

Therefore, it is important that the deployment of nodes takes account of installation height as well as horizontal distances. Since the WSNs for wildfire monitoring are deployed in area that is difficult to access, the power source has to support the long-term operation of a sensor node. The sensor node operates on limited battery power. When it dies and disconnects from the network the performance of the application is significantly affected. The sensors can take turns to sleep and work creating a balance in the energy consumption in order to maximize the WSN lifetime. Normal mode sensor node in each data active state works for 3s followed by is 7s-sleep, and thus the duty cycle is 0.3s.

A sensor node can perform sensing, receiving, and sending. The sequence of these operations is shown in Fig. 3.6. Sensing operation does not require the transceiver, and can therefore be performed in sleep state. After sensing, the node turns on its transceiver and goes into active state. It can then receive and process packets from neighboring nodes, also it can generate packets and send them to neighbor nodes. Nodes need to be synchronized with neighboring nodes, because the sender and the receiver must both be in active state to exchange packets. But if all the nodes are synchronized together, packet collisions are more likely to occur because all the nodes will attempt to send packets simultaneously.

For early wildfire detection there are vertical and horizontal techniques. The horizontal technique using surveillance of tower with human vision and video based monitoring[50], and vertical technique such as remote sensing technique. For remote sensing we can use satellite, unmanned aerial vehicles (UAV) or aircraft. These methods are based on the pictures takes, which enable us to monitor any potential fire. UAVs have been already deployed after several disasters [51], [57], [58] , installed camera was used to assess the situations. UAV flying up to 100 meters high takes pictures for ground information. In the case of wildfire verification and fire detection, it is important to have an accurate and up-to-date overview of situation. Hence, the observation areas covered by UAV provide for identification, control and verification of environmental conditions.

In recent years, there have been introduced some ideas from the field of unmanned aerial vehicles (UAVs). Surprisingly, UAVs are considered as sensor nodes with enhanced capabilities rather than as actuators. UAVs with specialized on-board sensor platforms can easily perform sensing and monitoring functions[59][60]. They can be also applied to target tracking and localization[61], [62]. As to their mobility, dedicated schemes for vehicle control and coordination have been proposed[63].

UAVs have also been considered for wildfire detection, which can be treated as a special case of monitoring and target tracking applications. A real-time algorithm for tracking the perimeter of fire has been proposed, however without testing it in practice [64]. Machines which are able to perform unmanned fire-fighting actions do not yet exist. However, with current aerial vehicle technology, they could be developed. There are also numerous types of specialized ground units, and new ones are being designed. Figure 3.8 shows a UAV route to visit all picture taking-points. This enables the planning of observation area, execution of mission and analysis of the video surveillance by UAV. During the UAV flight, we used infrared video and color camera to extract information of the covered area. The resulting image data from the UAV will be compared with the data from WSN to more accurately identify the fire hazard area.

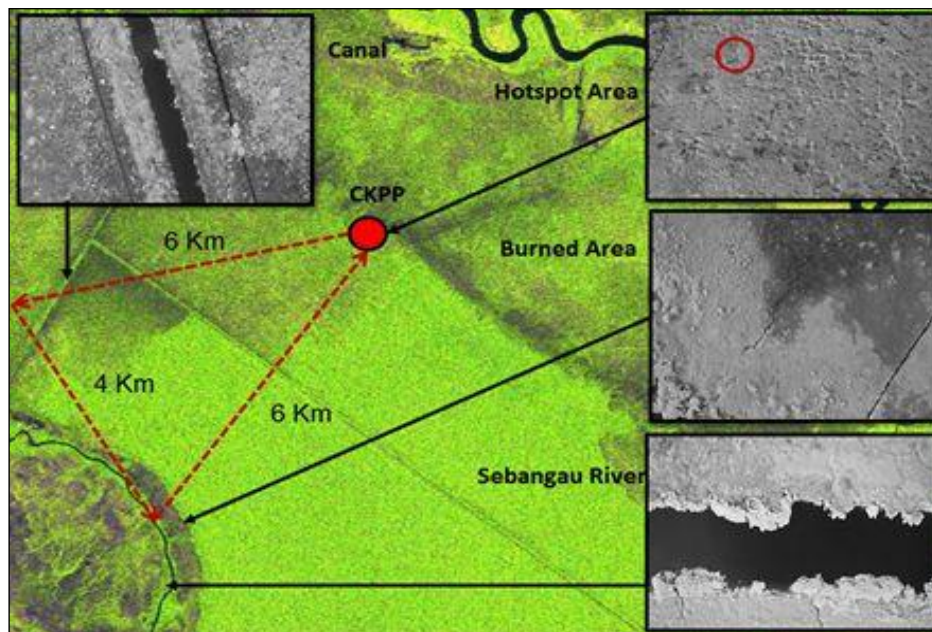


Figure 3.8: UAVs mission of observation area [7].

The location of the fire is very importance to fire-fighting patrols. To solve the problem, the sensor node should process to gain the knowledge of its physical location in space. UAV video surveillance is used for the verification of alert message from the sensor nodes as quick response of the fire detected by the sensor. Because combustion can occur at night, the light sensor and temperature are very useful information for the detection of wildfires at night. The accuracy and reliability of combination data WSN and UAV have large impact on peat fire detection. Sensor node can provide constant monitoring by low power consumption during the fire season. The potential fire reported from WSN is verified by the UAV to increase the reliability of the monitoring system.

3.3 Detection of potential fires

For experiment and implementation, WSN and UAV have been deployed to detect and monitor the peat forest in Central Kalimantan, Indonesia. As shown in Figure 3.6, the WSN includes 6 sensor nodes, gateway terminal and MoteView applications for monitoring. The distance between each sensor node is 100 meters, and the height of antenna sensor nodes from ground is 1.5 meters. Through this system we can detect a small fire of about three meters in size. In this study, sensor nodes deployed in peat forest environment, where the height of vegetation in the forest area ranges from 1 to 5 meters from the ground, which will affect WSN signal strength and radio propagation.

In the experiment, a small artificial fire was ignited for test the fire temperature sensor. The sensor will detect the change in temperature event of a fires. The wind direction will determine the heat transfer from the flame. Visual data sensor nodes will display on the base-station, when there are changes in temperatures. In reality, fire propagation is not so homogenous. The shape and velocity of a fire front, called the rate of spread[65], depends on a large number of factors, such as wind, terrain slope, topographic conditions, fuel (tree) type and moisture content, humidity and weather conditions.

Measurements acquired by sensors were transmitted to the base station which took the role of data storage and aggregation. In particular, measurements and their timestamps were stored in a SQLite database server running on Debian Linux operating system. Since the base station also provides the web server, clients can easily query the database at the remote system through the Internet. Fig. 3.9 shows the database page and the graphical interface page that are provided to the client. By using database, users may inquire about temperature and humidity for a specific node or for all nodes by specifying the time interval of interest. Moreover, the graphical user interface provides the state of all the nodes in the network and the most recent measurement acquisitions both numerically and graphically. Each sensor node normally operates in a normal mode, in which it periodically senses environmental data, and transfers the data to the sink node. The sensor monitors humidity as well as temperature in order to distinguish wildfire from high temperature. It also has to determine whether fire has broken out by analyzing the sensed temperature and humidity data. If fire is detected, the node immediately enters to alert mode, and sends messages to the sink node.

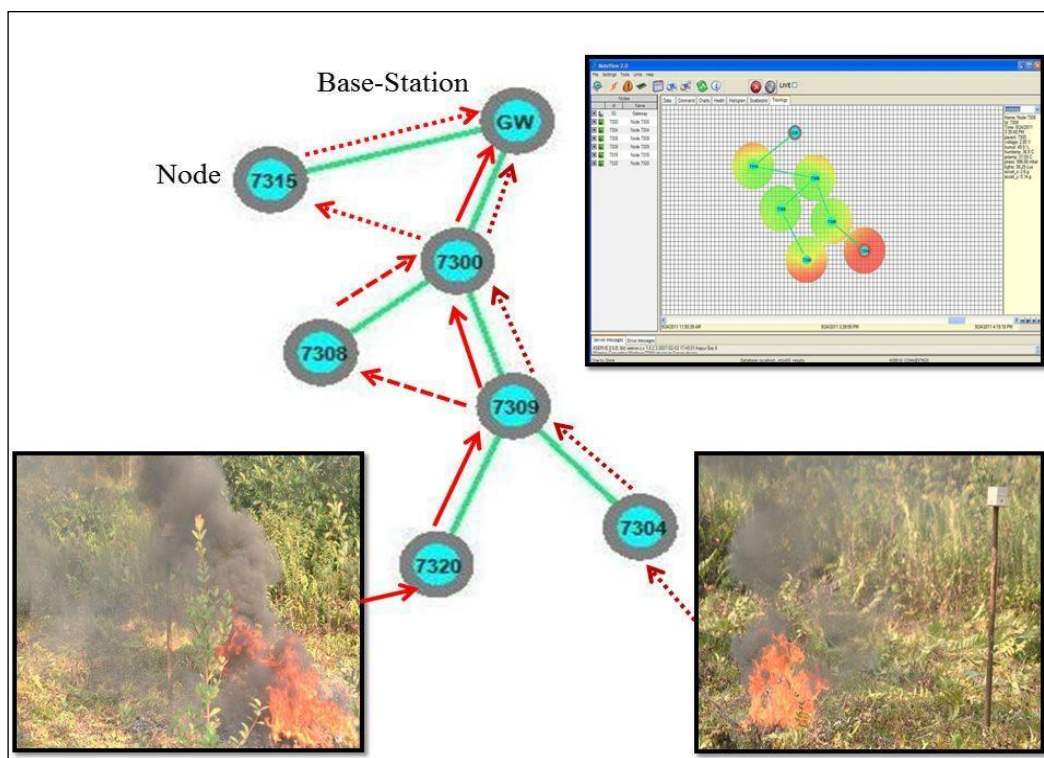


Figure 3.9: Flow of information fire WSN data

From the experiment, we obtained fire temperature data in forest area as shown in Fig 3.10 and Fig 3.11. What can be found from these figures are summarized as follows:

- There are sudden increase in temperature and sudden decrease in humidity for sensor #7304 at around 14:04 and 15:02,
- Maximum absolute temperature: 64 °C,
- Minimum absolute temperature: 30 °C,
- Average peak temperature: 46 °C.

In Central Kalimantan, the minimum temperature to be regarded as fire is 45°C, so that the temperature higher than 45°C is considered potential fire. The above measurement results strongly suggest that there are fires near #7304. Indeed, the artificial fires are ignited near #7304 at the times mentioned above.

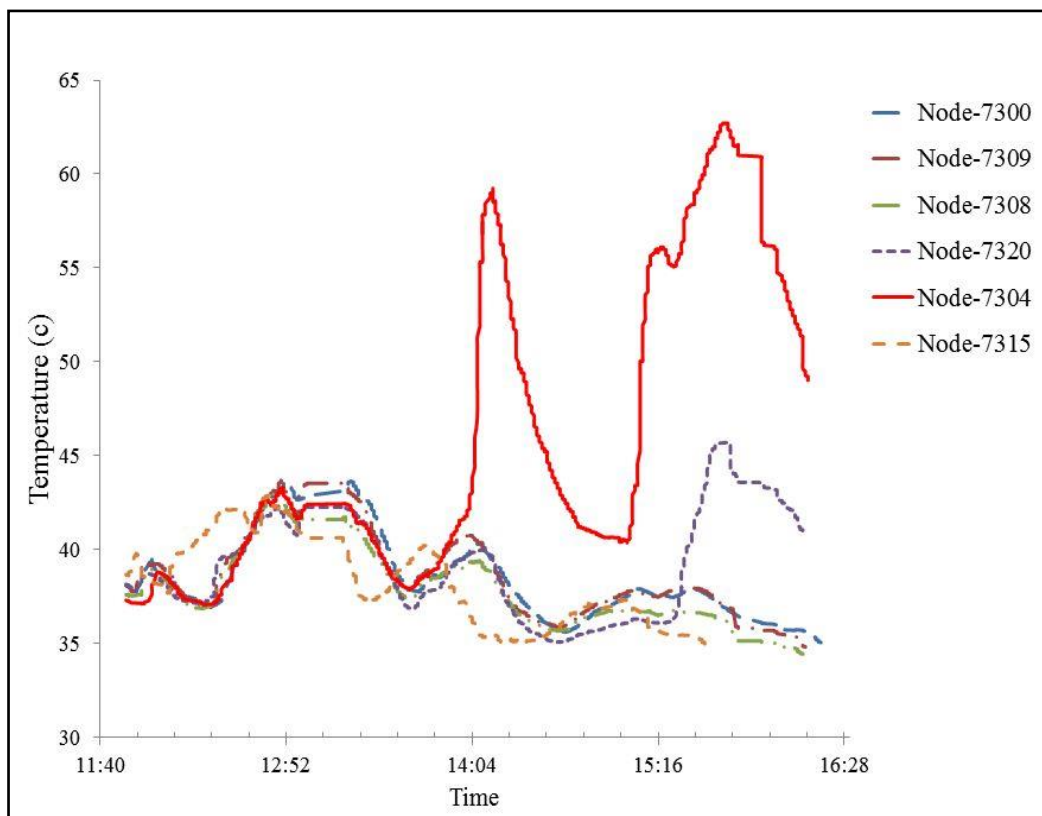


Figure 3.10: Temperature data detection of fire.

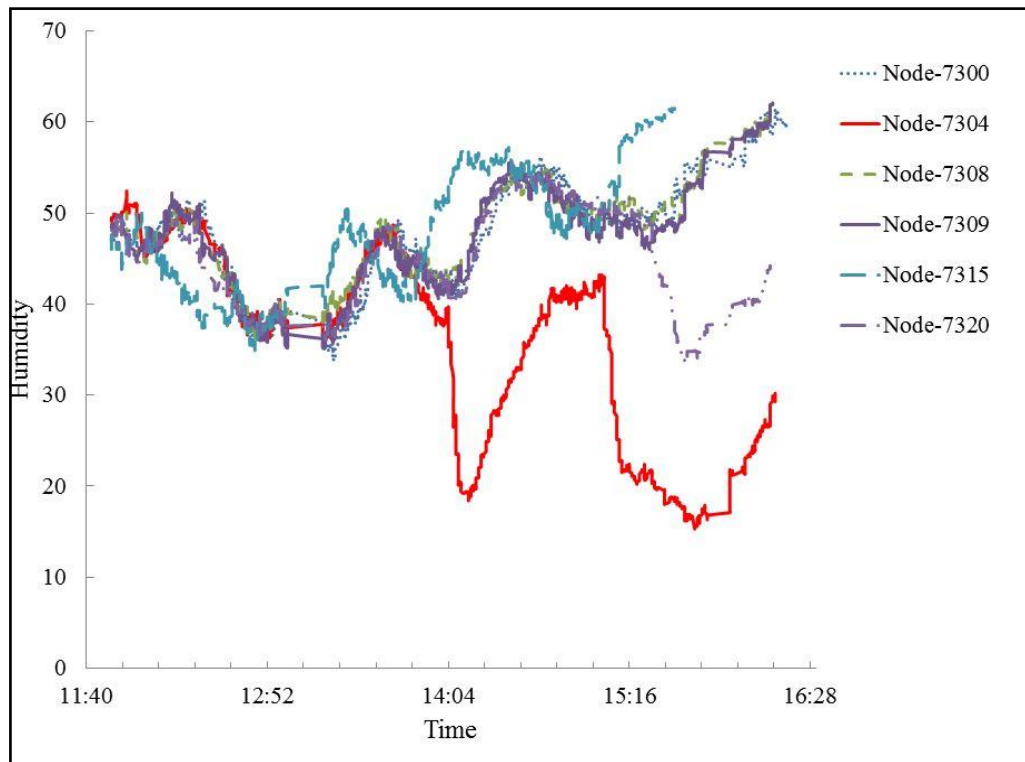


Figure 3.11: Humidity data detection of fire

3.4 Verification of potential fires

The locations of fire area are checked with the UAV video surveillance. The location of the fire is very importance to our fire patrols. To solve the problem, the sensor node should process to gain the knowledge of its physical location in space. UAV video surveillance is used for the verification of alert message from the sensor nodes as quick response of the fire detected by the sensor. Because combustion can occur at night, the light sensor and temperature are very useful information for the detection of wildfires at night.

In addition, Figure.3.12 shows the transmission of the fire temperature measured at sensor nodes to the base station, in which locations of fire area are checked with the UAV video surveillance. We compare the data measure by the WSN and UAV photo. The sensor #7304 detected sudden increases in temperature.

The UAV successfully found the corresponding fire near the sensor #7304. Moreover, the UAV also detected the other fire which caused increase in temperature measured by # 7320. In addition, the UAV could find the third fire which was not identified by the WSNs.

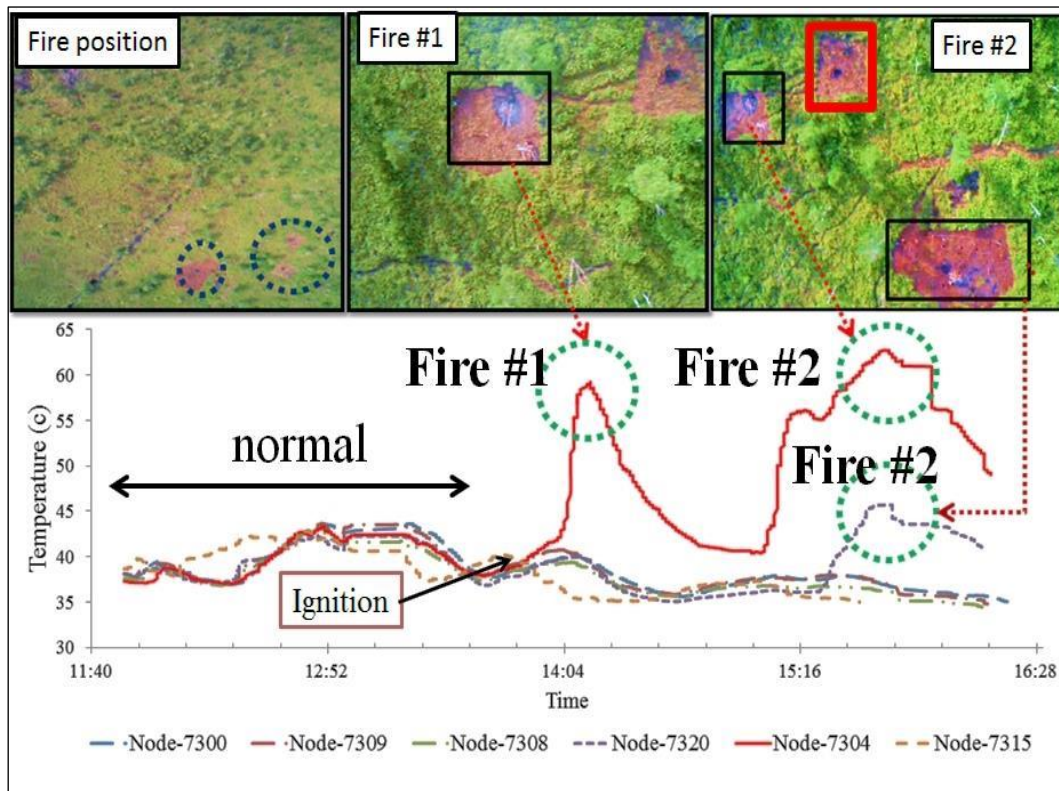


Figure 3.12: Comparison of data WSN with UAV photo

The accuracy and reliability of combination data obtained from WSN and UAV have significant impact on peat fire detection. Sensor node can provide constant monitoring by low power consumption during the fire season. On the other hand, UAV can perform observation of the potential fires detected by WSN even in fully smoke conditions. An integration of system composed of WSN and the UAV can detect fires which cannot be detected by the satellite due to their small spatial scale or smoky conditions.

3.5 Summary

What was concluded from this study is summarized as follows:

1. The UAV could fly to detect the potential fire informed by satellite.
2. The sensor networks detected sudden increase in temperature and sudden drop in humidity near the artificial fire.
3. The UAV could detect potential fire position and find the potential fire. This means that the system works very well.
4. The UAV could also find the fire which the WSN could not detect.

Chapter 4 Propagation of EM waves in forest

4.1 Radio propagation in forest

Models for the analysis of the propagation of electromagnetic waves through forest have been studied for a long time to understand the effects of the different elements of this complex medium. These effects depend largely on the frequency of the incident wave. At low frequencies (1-90 MHz), the dimensions of the elements of the canopy (small branches and leaves) are small compared to the wavelength, these elements are transparent to the incident wave and their effects are negligible on the propagating wave.

The forest medium is modeled by dielectric homogeneous layers representing the ground, the vegetation layer (trunks, branches), the air and the ionosphere [66][67]. For high frequencies (up to 500 MHz), all the elements of the medium need to be considered and are modeled by cylinders (trunks, branches) and ellipsoids (leaves). The scattered field from each element is calculated separately and added coherently or not to obtain the total scattered field [68].

Since the forest is a random medium with many discrete scatter such as the randomly distributed leaves, branches and tree trunks, radio waves propagating in the forest naturally experiences multiple scattering, diffraction, and absorption of radiation. These different propagation mechanisms, when combined, can result in severe fades in the received signal, and produce an excess vegetation induced loss as compared to terrestrial propagation. These fade effects have to be considered in order to establish a highly reliable near ground communication link.

In WSNs based on the Zigbee protocol, measured data are sent by ultra-high frequency (UHF) band electromagnetic waves from sensor nodes to routers or directly to the base station. The routers gather measured data from the forest and send them to the base station via multihop communication. One of the largest problems in operation of WSNs is their energy constraints: the

sensor and router nodes usually have limited energy source such as batteries and solar panels. It is impractical to make frequent replacement of the batteries in the sensor nodes widely deployed in forests. Moreover, sufficient energies for proper operation of the sensor nodes cannot be provided from the batteries charged by the solar panels in rainy season.

For the communications inside the forest, the distance between transmitter and receiver is much larger than the wavelength so that the fields in the stratified structure are described by only the lateral wave on the air side along the air-canopy interface. In reliable modern, communication system is very important and significant for the implementation WSN in forest and vegetation environment.

In this study, optimization method based on simulated annealing (SA)[69] for deployment of routers of Zigbee-based WSN whose working frequency is in UHF band. In particular, where consider the WSNs located in inhomogeneous lossy media such as forest and grassland.

4.1.1 Propagation modes in forest

There are three electromagnetic wave contributions to the field [66] [70]: geometric optical waves propagate directly or reflectively from the source to the sink through the tree trunks and canopy. The sky waves have long triangular path whose vertexes are the source, sink and ionosphere. Moreover, the lateral waves propagate along the canopy-air interface. In this study can discard the second waves for WSNs because they use UHF waves which do not have reflection from the ionosphere.

The first and third waves vary with distances as $\exp(-\alpha x)/x$ and $1/x^2$. Hence it depends on the distance and the attenuation constant α of the medium which wave is dominant. A full wave analysis based on four layer model of the forest concludes that the former is dominant above 100 MHz if the communication distance is shorter than 3 km [71].

In the WSNs for forest fire detection, the communication distance of the sensors and routers would be sufficiently shorter than 3 km. For this reason, in this study only consider the first

waves (see Fig. 4.1). Moreover, for simplicity, in this study only consider the direct waves. It is possible to consider reflection from ground surface into account on the basis of two-ray ground reflection model in the following analysis.

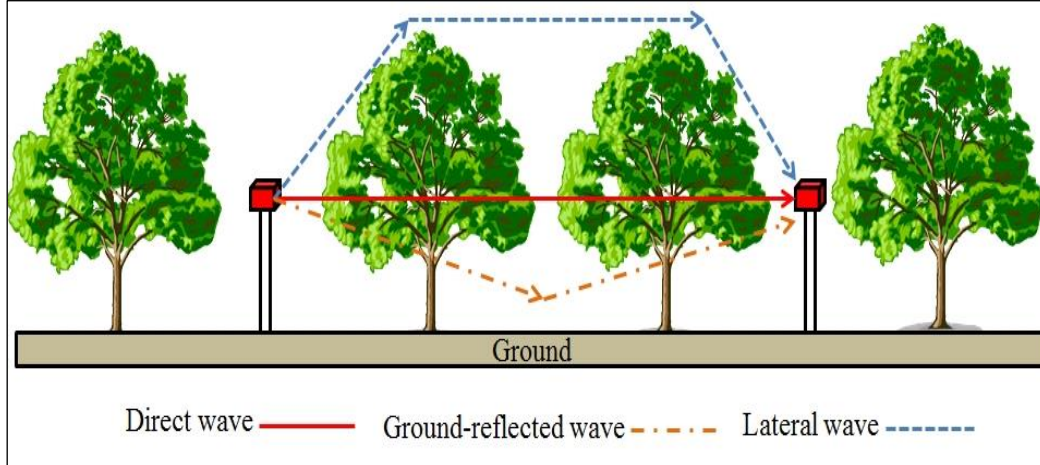


Figure 4.1: Radio wave propagation in the forest

4.1.2 Electromagnetic waves in absorbing media

Let us consider electromagnetic waves in inhomogeneous lossy dielectric media, which are governed by the Maxwell equations

$$\text{rot } \mathbf{E} = -j\omega\mu_0 \mathbf{H}, \quad (4.1)$$

$$\text{rot } \mathbf{H} = j\omega\hat{\epsilon} \mathbf{E}, \quad (4.2)$$

where $\mathbf{E}, \mathbf{H}, \omega, \mu_0$ are electric field, magnetic field, angular frequency and permeability in vacuum. Moreover $\hat{\epsilon}$ is the complex permittivity defined by

$$\hat{\epsilon} \equiv \epsilon_0 \epsilon_r - j \frac{\sigma}{\omega}, \quad (4.3)$$

where $\epsilon_0, \epsilon_r, \sigma$ are permittivity in vacuum, relative permittivity and conductivity, and j denotes the imaginary unit.

In this study make here following assumptions on the dielectric property of the medium:

- The loss is dominant so that $\sigma/(\epsilon_0 \epsilon_r \omega) \ll 1$.
- The relative permittivity ϵ_r is uniform while conductivity σ varies with position.

(c). The spatial scale of σ is sufficiently smaller than the wavelength of UHF wave $2\pi/k_r$. That is, assuming that σ varies sinusoidally, $\sigma = \sigma_0 \exp(jk_\sigma r)$, the magnitude of $d\sigma/dr$ is expressed by $\sigma_0 k_\sigma$ which is sufficiently smaller than $\sigma_0 k_r$.

Now introducing vector potential satisfying, $\mathbf{H} = \text{rot}\mathbf{A}/\mu_0$, which obeys the Lorentz gauge, the vector Helmholtz equation

$$\nabla^2 \mathbf{A} + \dot{k}^2 \mathbf{A} = 0, \quad (4.4)$$

can be derived from (4.3)(4.2), where \dot{k} is the complex wave number defined by

$$\dot{k} = \sqrt{\omega^2 \mu_0 \dot{\epsilon}}. \quad (4.5)$$

Due to the assumption (a), \dot{k} can be approximated as

$$\begin{aligned} \dot{k} &\approx k_0 \sqrt{\epsilon_r} \left(1 - \frac{j}{2} \frac{\sigma}{\epsilon_r \epsilon_0 \omega} \right) \\ &\equiv k_r - j\alpha. \end{aligned} \quad (4.6)$$

For simplicity, this study has consider a wave radiated from a dipole in z direction perpendicular to ground, which is governed by the one-dimensional scalar Helmholtz equation given by

$$\frac{d^2 f}{dr^2} + [k_r^2 - 2jk_r \alpha(r)]f = 0, \quad (4.7)$$

where $f(r) = rA_z$.

It can be shown that the damped wave solution

$$f(r) = C e^{-jk_r r} e^{-\int \alpha(r) dr}, \quad (4.8)$$

satisfies (4.7) under the assumptions (a)-(c). Note that (4.8) is an exact solution to (4.7) when α is constant.

It is therefore concluded that the vector potential is given by

$$A = \frac{C e^{-jk_r r} e^{-\int \alpha(r) dr}}{r} \hat{z} \quad (4.9)$$

It can also find that E and H also have the spatial attenuation of the form $\exp(-\int \alpha(r) dr) / r$.

4.1.3 Modeling of electromagnetic waves in forest

In this study we consider the WSN in peat forest shown in Fig.4.2 which is composed of burned and unburned forest. The regions P1, P2 and P3 have different values of basal area; 28.6, 18.73 and 18.43 m^2ha^{-1} [74]. The sensing field of interest would also contain river and grassland. The regions have to consider different attenuations in wave propagation in these fields.

Basal area is the term used in forest management that defines the area of a given section of land that is occupied by the cross-section of tree trunks and stems at their base. In most countries, this is usually a measurement taken at the diameter at breast height (1.3m or 4.5 ft) of a tree above the ground and includes the complete diameter of every tree, including the bark. Measurements are usually made for a plot and this is then scaled up for 1 hectare of land for comparison purposes to examine a forest's productivity and growth rate.

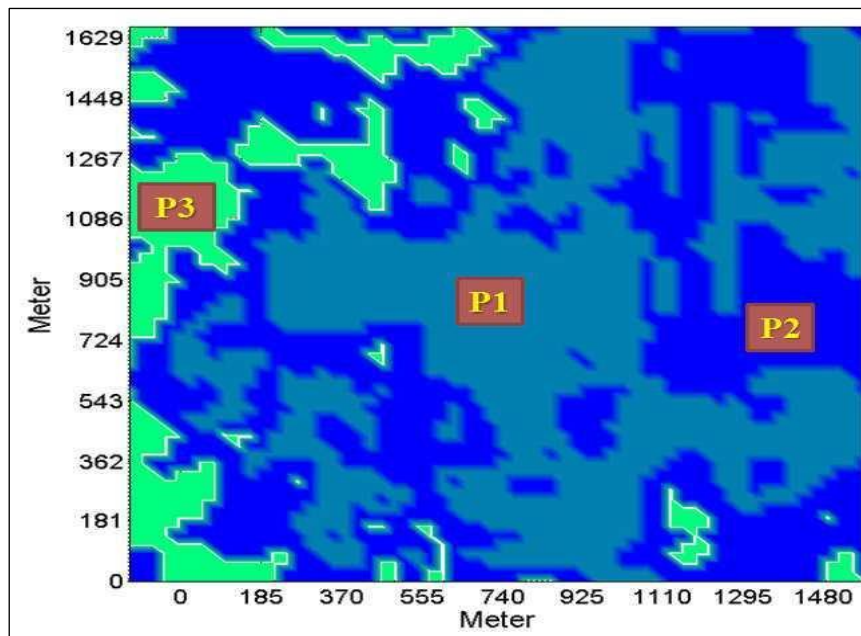


Figure 4.2: Sensing field in tropical peat forest in Central Kalimantan, Borneo

It has been pointed out in [66], [70] that the electromagnetic waves in forest can be classified into geometric optical waves which propagate directly or reflectively from the source to the sink through the tree trunks and canopy, the sky waves which have long distant propagation from a source to sink in forest via ionosphere, and finally the lateral waves which propagate along the canopy-air interface. We can discard here the second waves for WSNs at UHF band in which electromagnetic waves have negligible reflections from the ionosphere. The first and third waves vary with distances as $\exp(-\alpha x)/x$ and $1/x^2$, respectively. A full wave analysis based on four layer model of the forest has concluded that the former is dominant above 100 MHz if the communication distance is shorter than 3 km[71]. In the WSNs for forest fire detection, the communication distance of the sensors and routers would be sufficiently shorter than 3 km. For this reason, we consider only the first waves in this study. Moreover, for simplicity, we only consider the direct waves. It is possible to consider reflection from ground surface into account on the basis of two-ray ground reflection model in the following analysis.

In the analysis of electromagnetic waves in forests which are regarded as inhomogeneous dielectric media, we make the following assumptions.

- (a) The electromagnetic property of the forest which is composed of tree trunks and air, and we can introduce the homogenized complex permittivity given by (4.3). where ε and σ are homogenized permittivity and electric conductivity of forest, respectively, and ω denotes angular frequency. Because there are various vegetation in the sensing field as written above, ε and σ are treated as function of position.
- (b) The forest is lossy dielectric which satisfies

$$\tan \delta \equiv \frac{\sigma}{\varepsilon\omega} \ll 1, \quad (4.10)$$

where δ is a loss angle.

- (c) The characteristic length of ε and σ is sufficiently longer than the wavelength of UHF wave.

4.1.4 Homogenized permittivity of forest

In the homogenization we define the homogenized material constants such as permittivity and permeability which relate electromagnetic field quantities such as \mathbf{E} and \mathbf{D} averaged over heterogeneous materials. The homogenization technique is particularly effective for analysis of composite materials, and its validity has been verified in many cases [e.g. 76]. There are two kinds of homogenization techniques; analytical approach in which mutual interaction between the particles is assumed weak and linear, and numerical approach which considers the strong and nonlinear mutual interaction into account [75].

For the analysis of electromagnetic waves in forest, in this study we employ the analytical approach assuming that the density of trees is sufficiently low. In fact, the basal area is lower than 1% of the sensing field in the case of Fig.4.2.

In the following, homogenized permittivity will be derived with reference to [76] in which shielding effectiveness of epoxy resin filled with carbon fibers is discussed. Note that homogenization has never been applied to analysis of electromagnetic wave propagation in forest. In this simulation is consider the constitutive relation of electric field in a tree trunk which is given by

$$\mathbf{D}_i = \epsilon_0 \mathbf{E}_i + \mathbf{P}_i = \epsilon_i \mathbf{E}_i \quad (4.11)$$

where i indexes materials including air. Hence the polarization vector can be expressed as

$$\mathbf{P}_i = (\epsilon_i - \epsilon_0) \mathbf{E}_i. \quad (4.12)$$

On the other hand, the electric field \mathbf{E}_P generated by \mathbf{P} outside the tree trunk is given by

$$\epsilon_0 \mathbf{E}_P = N \mathbf{P}_i, \quad (4.13)$$

Where N denotes the depolarization constant which only depends on geometry of the dielectric material. On the surface of the tree trunk, the boundary condition

$$\mathbf{E}_i = \mathbf{E}_0 - \mathbf{E}_P, \quad (4.14)$$

Must hold, where \mathbf{E}_0 is the mean external field to which \mathbf{E}_p is antiparallel. From (4.12)-(4.14), it follows that

$$\mathbf{E}_i = \frac{\varepsilon_0 \mathbf{E}_0}{\varepsilon_0 + N(\varepsilon_i - \varepsilon_0)} . \quad (4.15)$$

Now the homogenized constitutive relation for averaged field can be expressed as

$$\begin{aligned} \langle \mathbf{D}_i \rangle &= \tilde{\varepsilon} \langle \mathbf{E}_i \rangle \\ &= \varepsilon_0 \left\langle \frac{1}{\varepsilon_0 + N(\varepsilon_i - \varepsilon_0)} \right\rangle \mathbf{E}_0 . \end{aligned} \quad (4.16)$$

On the other hand, taking spatial average of (4.11), we obtain

$$\begin{aligned} \langle \mathbf{D}_i \rangle &= \langle \varepsilon_i \mathbf{E}_i \rangle \\ &= \varepsilon_0 \left\langle \frac{\varepsilon_i}{\varepsilon_0 + N(\varepsilon_i - \varepsilon_0)} \right\rangle \mathbf{E}_0 . \end{aligned} \quad (4.17)$$

It follows from (4.16) and (4.17) that the homogenized permittivity is given by

$$\tilde{\varepsilon} = \frac{\left\langle \frac{\varepsilon_i}{\varepsilon_0 + N(\varepsilon_i - \varepsilon_0)} \right\rangle}{\left\langle \frac{1}{\varepsilon_0 + N(\varepsilon_i - \varepsilon_0)} \right\rangle} . \quad (4.18)$$

When it considers the medium composed of tree trunks whose complex permittivity is $\dot{\varepsilon}$ and air, it can obtain the homogenized permittivity of forest from (4.18) as follows:

$$\tilde{\varepsilon} = \varepsilon_0 + \frac{\varepsilon_0(\dot{\varepsilon} - \varepsilon_0)f}{\varepsilon_0 + N(1-f)(\dot{\varepsilon} - \varepsilon_0)} , \quad (4.19)$$

Where $0 \leq f \leq 1$ is the volume fraction of tree trunks.

When the electric field has polarization parallel to the tree trunks, we find that $N \approx 0$ assuming that tree can be treated as an infinite cylinder. On the other hand, it is found that $N \approx 1/2$ when the polarization is perpendicular to the trees. Hence the permittivity for each case is given by

$$\tilde{\varepsilon}_{\parallel} = (1 - f)\varepsilon_0 + f\dot{\varepsilon} , \quad (4.20)$$

$$\tilde{\varepsilon}_{\perp} = \varepsilon_0 + \frac{2\varepsilon_0(\dot{\varepsilon} - \varepsilon_0)f}{2\varepsilon_0 + (1-f)(\dot{\varepsilon} - \varepsilon_0)} . \quad (4.21)$$

It has been shown in [76] that the shielding effectiveness of a composite material computed by FEM using the homogenized permittivity in (4.20)-(4.21) agrees well with that computed by FEM without homogenization. Note that the latter FE analysis needs a number of elements to model the fine structure of the composite material. When $f \ll 1$, which would hold for forests, (4.20)-(4.21) reduces to

$$\tilde{\epsilon}_{\parallel} \approx \epsilon_0(1 - jf \tan \delta) , \quad (4.22)$$

$$\tilde{\epsilon}_{\perp} \approx \epsilon_0 \left\{ 1 - j \frac{4f \tan \delta}{\left(1 + \frac{\epsilon}{\epsilon_0}\right)^2} \right\} . \quad (4.23)$$

From (4.23), we can obtain the homogenized conductivity, which is inserted into (4.6) to have the homogenized attenuation constants

$$\tilde{\alpha}_{\parallel} \approx \frac{1}{2} f \omega \sqrt{\epsilon_0 \mu_0} \tan \delta , \quad (4.24)$$

$$\tilde{\alpha}_{\perp} \approx \frac{2f \omega \sqrt{\epsilon_0 \mu_0}}{\left(1 + \frac{\epsilon}{\epsilon_0}\right)^2} \tan \delta . \quad (4.25)$$

Equations (4.24)-(4.25) are valid under assumption (4.25). It is clear from (4.24)-(4.25) that

$$\frac{\tilde{\alpha}_{\parallel}}{\tilde{\alpha}_{\perp}} \approx \frac{1}{4} \left(1 + \frac{\epsilon}{\epsilon_0}\right)^2 > 1. \quad (4.26)$$

We can conclude, therefore, that the attenuation constant for the perpendicular polarization is smaller than that for the parallel polarization.

4.2 Computation of attenuation constants

First let us consider a uniform field where α is constant. The communication distance R in this field can be obtained by solving the nonlinear equation

$$\frac{e^{-\alpha R}}{R} = \frac{1}{R_0} . \quad (4.27)$$

The communication distance is plotted for different values of R_0 (free-space) as a function of α in Fig. 4.3. Shown estimate the number of routers N necessary for full coverage of the sensing field of area $A[m^2]$ from

$$N = \frac{A}{\pi R^2}. \quad (4.28)$$

Figure 4.4 shows dependence of N on α and R_0 .

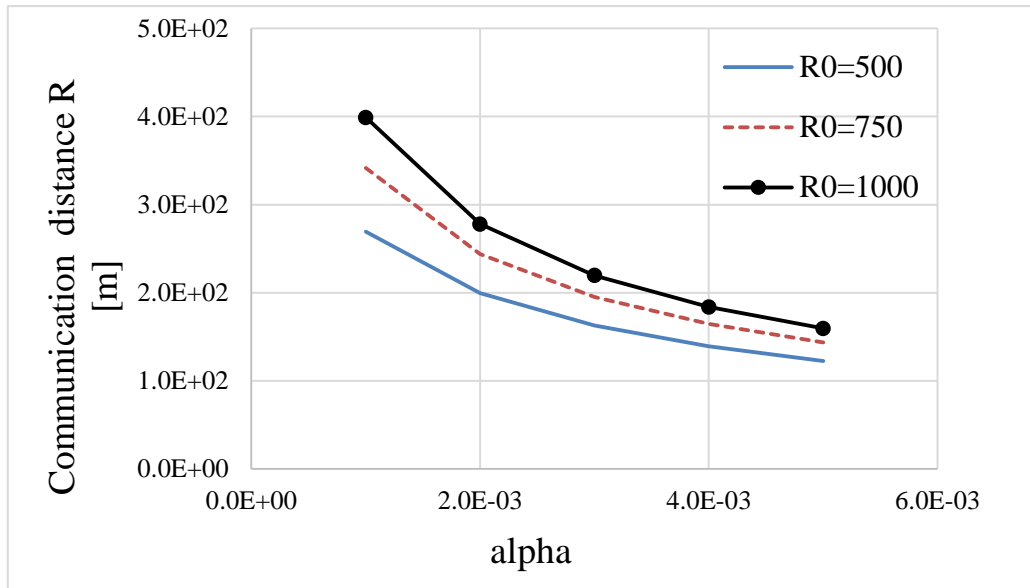


Figure 4.3: Communication distance R in lossy sensing field

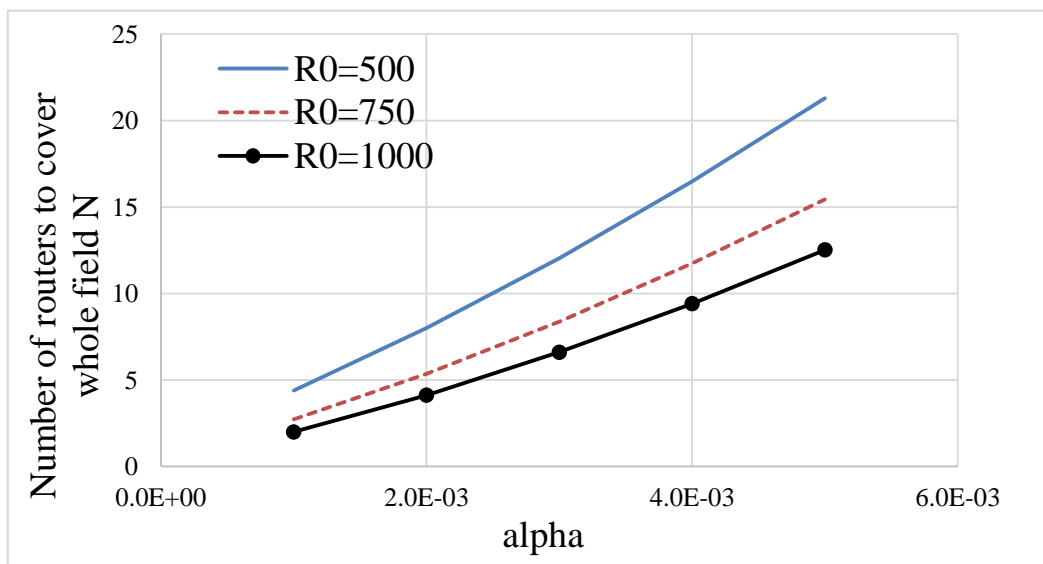


Figure 4.4: Number of routers N for full coverage of sensing field of $10^6 m^2$. R_0 [m] represents communication distance in free space.

The complex permittivity $\hat{\epsilon}$ of tree trunks in tropical forest has been measured [77]. Although depends on the kind of tree trunk, we assume that $\hat{\epsilon} = \epsilon_0(3.1 - j0.4)$ which has been used for scattering analysis of single tree trunk in [77]. Figure 4.5 shows dependence of the attenuation constants of parallel and perpendicular polarization on frequency for P2 forest. It can be seen that they approach the values given by the formula (4.23)-(4.24) as frequency increases. At low frequencies where assumption (4.24) is no more valid, $\tilde{\alpha}_\perp$ takes smaller values.

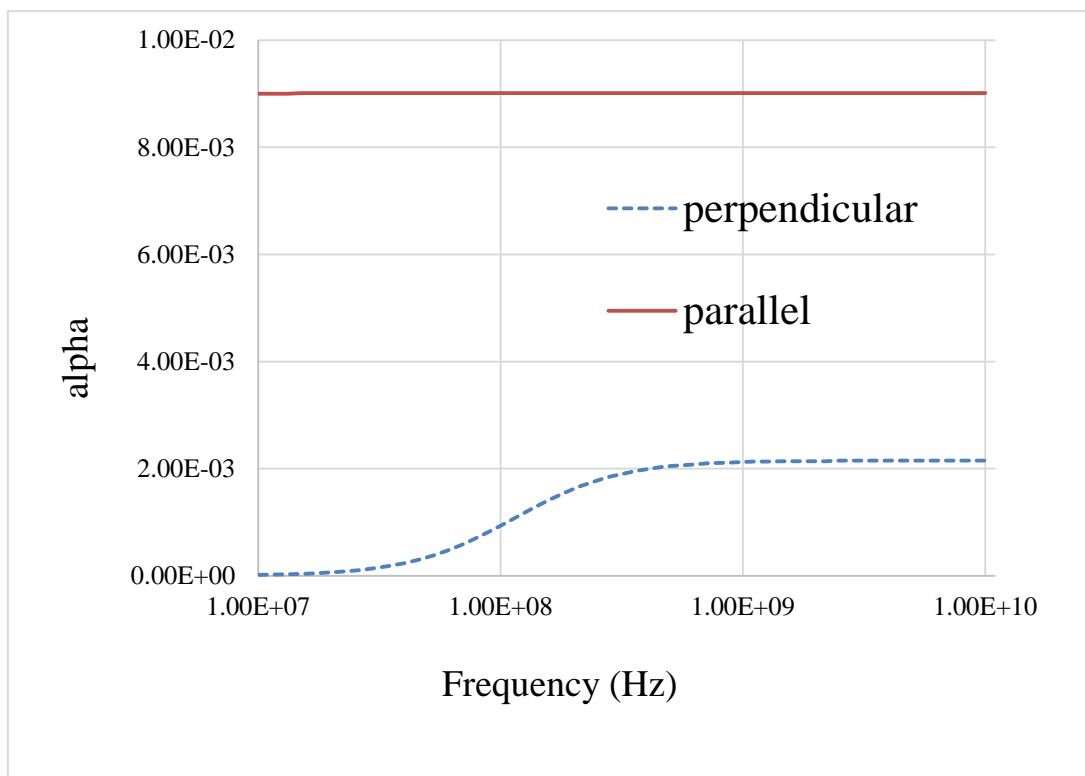


Figure 4.5: Attenuation constants in P2 for different polarization

Chapter 5 Optimization of WSN in forest

In this chapter, we discuss the optimization of WSN topology in forest based on the results mentioned in the previous chapter. That is, in the optimization, the attenuation of the electromagnetic waves in the forest is evaluated by the homogenization technique to determine the connectivity between the nodes in WSN. In the following, after the optimization method is described, the optimization results will be reported in detail.

5.1 Optimization method

In this section, the optimization method is described. First I describe how to determine the connectivity of sensor and router nodes considering the attenuation of electromagnetic waves in the forest. Next, I explain how to determine the network topology of the WSN. Finally, the optimization method for router deployment using the simulated annealing is described.

5.1.1 Formation of wireless sensor networks

In the optimization, we adopt the following assumptions for determination of wireless sensor networks topology for simplicity.

- (a). The sensors, routers and base station have a common threshold in electric field E_0 above which they communicate with others.
- (b). The multi-hop transmission is available for the routers but not for sensors. The magnitude of electric field which is generated by node i and received by node j , and vice versa, is expressed by $E_{ij} = \exp\left(-\int_{C_{ij}} \alpha(r) dr\right) / d_{ij}$, where C_{ij} and d_{ij} denotes a straight line connecting these points and their distance.

5.1.2 Wireless sensor networks deployment algorithm

The WSN topology is determined from the following algorithm.

- (1) The tentative layer level, say -1, is given for all the routers.

- (2) The sensor i and its nearest node j which is either a router or base station are connected if $E_{ij} \geq E_0$.
- (3) The router i and its nearest base station j are connected if $E_{ij} \geq E_0$. The layer level of the connected router is set to 1 and the current layer level L is set to 1. Then the following procedure is repeated until there are no routers which can be connected to the other routers.
- (4) The router i of level $L-1$ and its nearest router j of level L are connected if $E_{ij} \geq E_0$. If router i is connected, then its layer is set to $L + 1$.
- (5) $L = L + 1$. Return to (4).

5.1.3 Optimization using simulated annealing

The objective function to be maximized is just equal to the number of connected sensors, N . For optimization of WSN topology, this study employ the simple SA (simulated annealing) [72] whose algorithm is described below.

1. Set the values of δ , $0 \leq P_{th} \leq 1$, $0 \leq \gamma \leq 1$, initial temperature T_0 and maximum iteration count M . N_s sensors and N_r routers are randomly deployed in the target field Ω .
2. One router is randomly chosen and its position $\mathbf{x} = (x, y)$ is modified to $\mathbf{x}' = (x + \delta a, y + \delta b)$, where $0 \leq a, b \leq 1$ are random numbers and δ is a given constant. If \mathbf{x}' is outside of Ω , this modification is discarded. The topology of both WSNs is determined using the algorithm described in section 4.2.1, and the numbers of connected sensors, N, N' , are computed.
3. If $\Delta N = N' - N$ is positive, then this modification is accepted. Otherwise, the algorithm compute $P = \exp(\Delta N/T)$. If $P \geq P_{th}$ ($P < P_{th}$), then the modification is accepted (rejected).
4. The temperature is decreased by $T = \gamma T$. If iteration count is smaller than M , then return to (2).

5.2 Optimization results

5.2.1 Artificial test problem

In this study we apply the present optimization method to an artificial test problem, where an area of highly attenuation with $\alpha=1/100$ is located near the base station. In all the optimization mentioned below, the optimization parameters are set as follows: $E_0=1/300$, $SN=30$, $\delta=20$, $P_{th}=0.5$, $M=1000$, $T_0=1$. It is expected that the WSN topology would be formed avoiding the attenuation area. Figure 5.1 shows the optimization result.

In figure 5.1 can see that all the sensors are successfully connected to their parent nodes and their communication routes detour around the attenuation area, as expected.

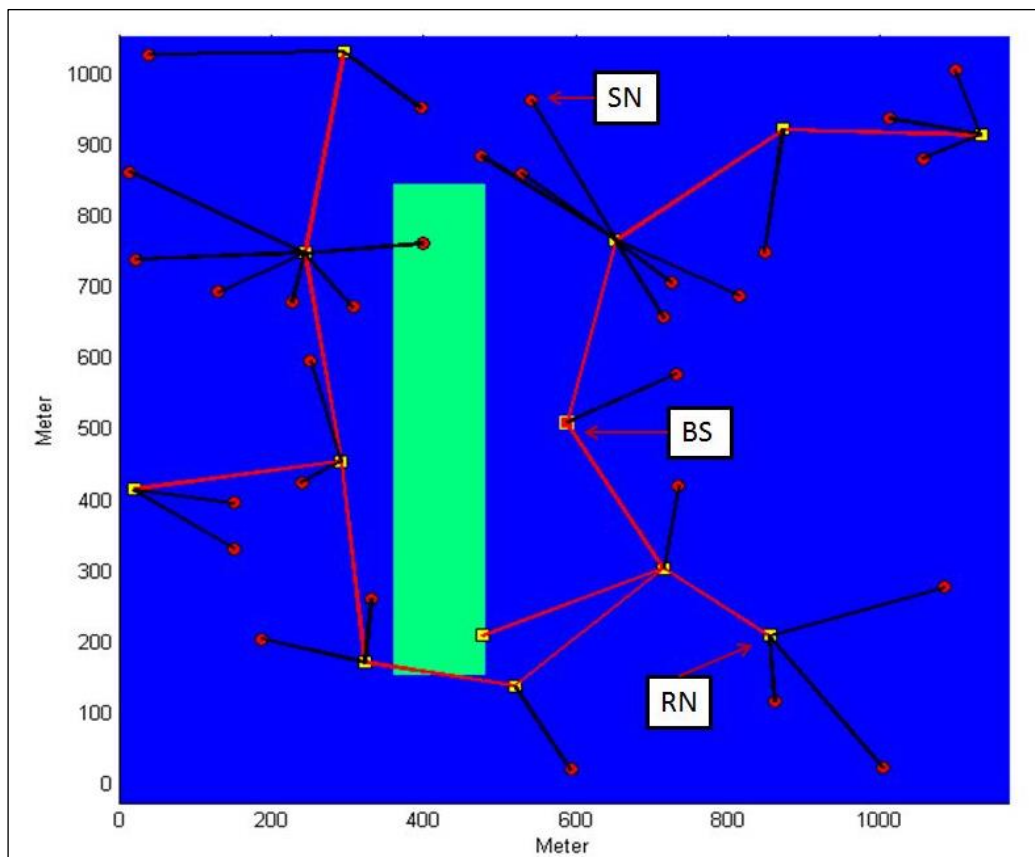


Figure 5.1: Artificial problem with attenuation area with $\alpha=1/100$ near base station, $RN=12$

5.2.2 Optimization of WSN for assumed attenuation constants

In this study, for the real problem area we choose the tropical rain forest in Central Kalimantan, Indonesia for a case study of the simulation. The map of the location is obtained from Landsat images (see Fig. 5.2). There are forest, grassland and free space. The map is generated using the System for Automated Geoscientific Analyses (SAGA) [85] to extract the information about forest and vegetation from Landsat images. We also perform optimization of a free space with the same area for comparison. In these models, the sensors and router nodes are placed randomly and the latter positions are optimized.

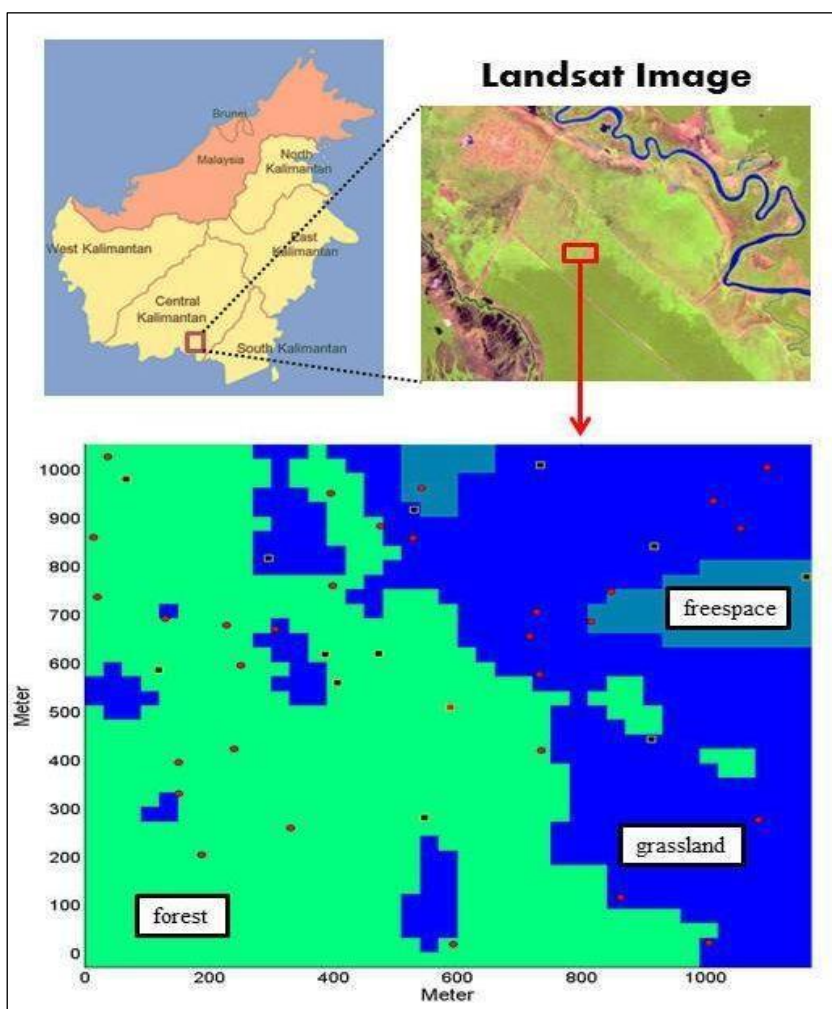


Figure 5.2: Location of tropical rain forest site in Central Kalimantan, Borneo

In this study we use the same random seed for both optimizations. To evaluate the electric field received by the nodes, which depends on α defined in (4.5), we need the values of the homogenized permittivity ϵ_r and electric conductivity σ for forest and grassland. According to [70], their ranges are $1.01 \leq \epsilon_r \leq 1.5, 10^{-3} \leq \sigma \leq 10^{-5}$ S/m.

In [66], ϵ_r is assumed to be unity. Hence α would range from about 0.2 to 1.5×10^{-3} . Thus we assume here that $\alpha=1/600$ for forest. In [73], the received power P is assume to be of the form $P = P_0 - n \log(d_{ij})$ in dBm, and the values of n , determined by experiments, are compared for forest and grassland. At 2.45 GHz, the resultant value is 2.89 for pine forest, and it ranges from 3.55 to 4.13 for grassland in long communication.

Since their decay model is different from our exponential model, the value cannot evaluate α from these results for grassland. We assume that the decay for grassland is two times stronger than that for forest, that is $\alpha=1/300$ (see Fig 5.3). Note that the present optimization can be executed for arbitrary values of α .

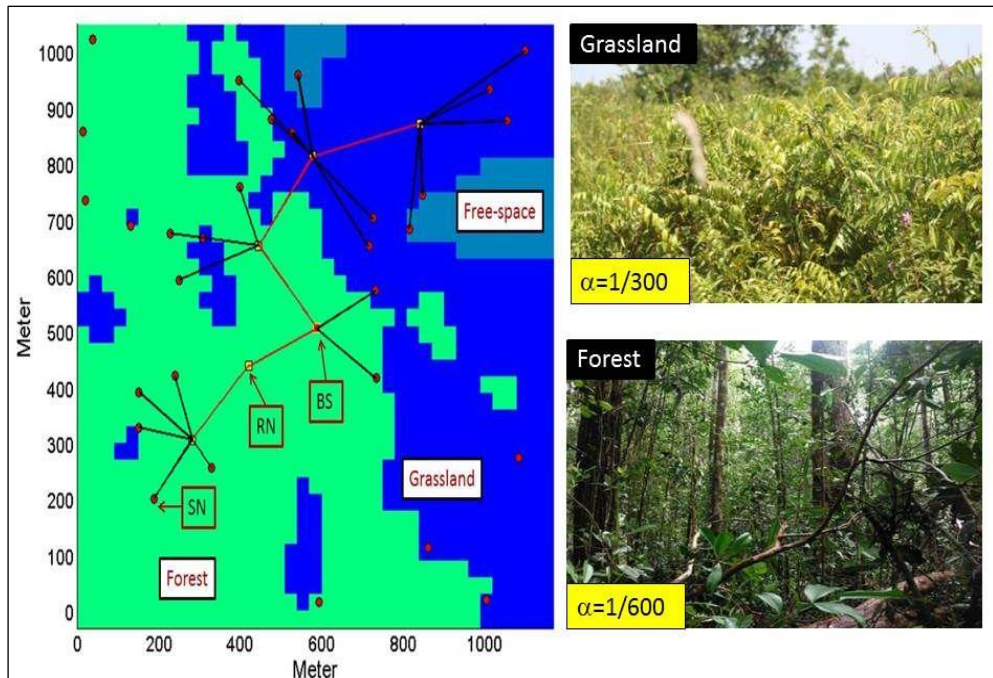
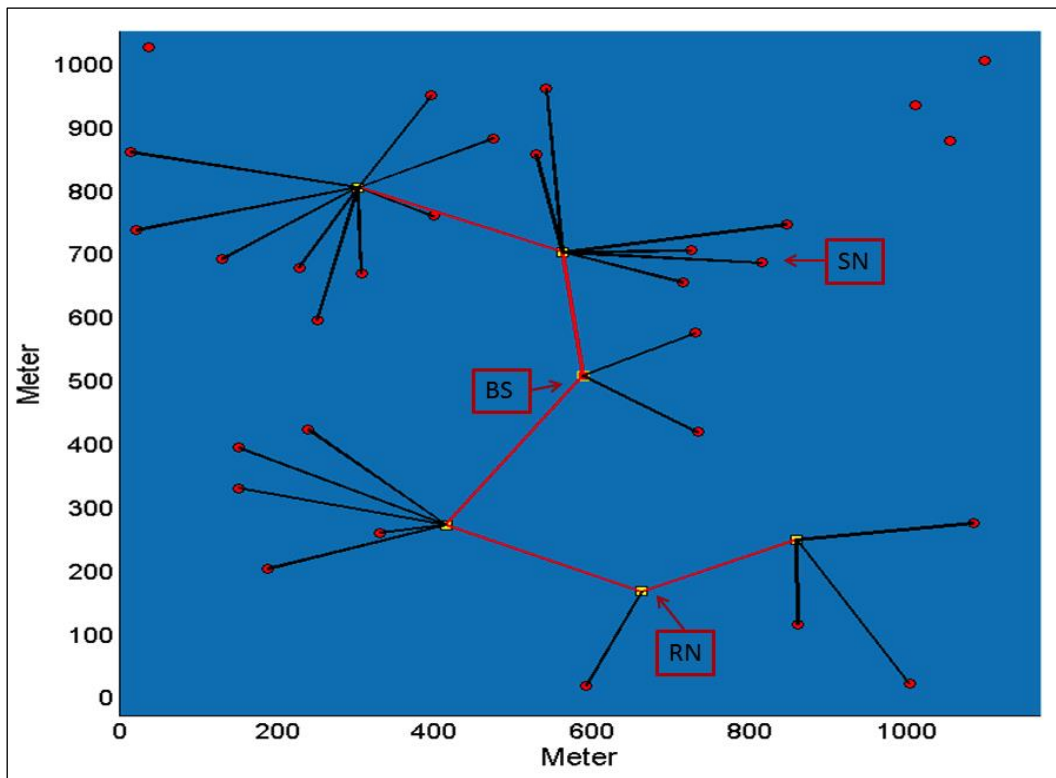


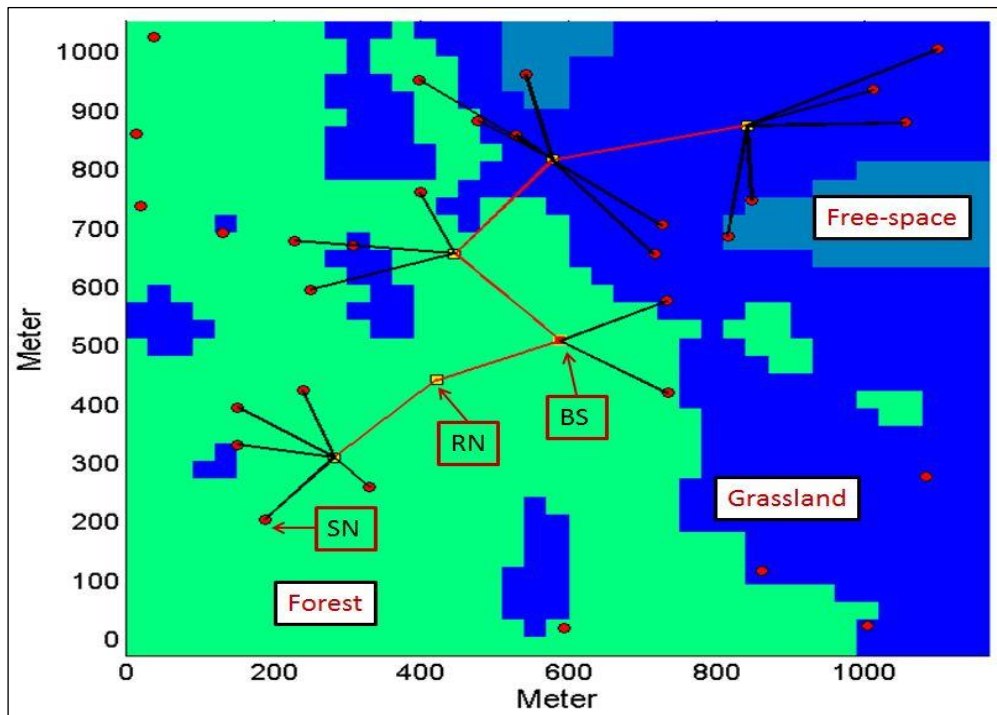
Figure 5.3 Sensing field in grassland and forest

Figure 5.4 shows the optimized WSNs when $RN=5$. In the simulation can find that the number of connected sensors is 26 and 22 for the free space and inhomogeneous area composed of forest, grassland and free space. Because of the stronger attenuations in the forest and grassland, the number of connected sensors is reduced for the latter case. Moreover, it can find the optimized network topology is different from each other.

Figure 5.5 shows the convergence histories of simulated annealing for both cases. After the initial fluctuations due to random search at high temperature, the values of the objective function (number of connected sensors) almost monotonously increase and converge to the final values.



(a) Free space



(b) Inhomogeneous field composed of forest, grassland and free space

Figure 5.4: Optimized results for RN=5

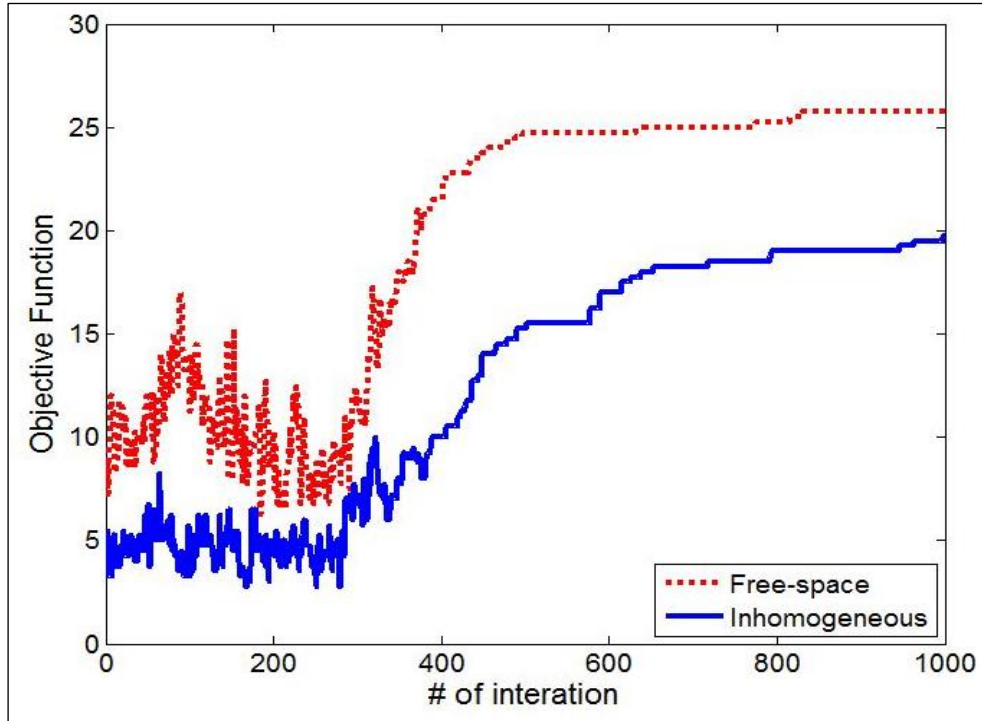
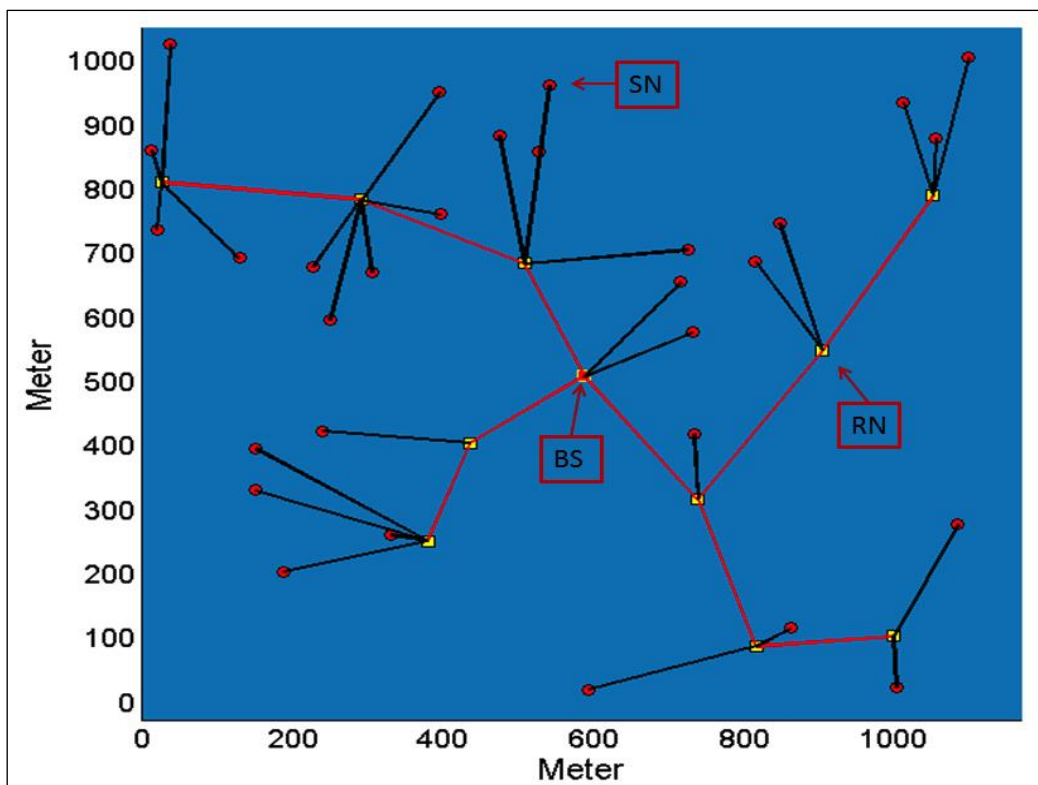


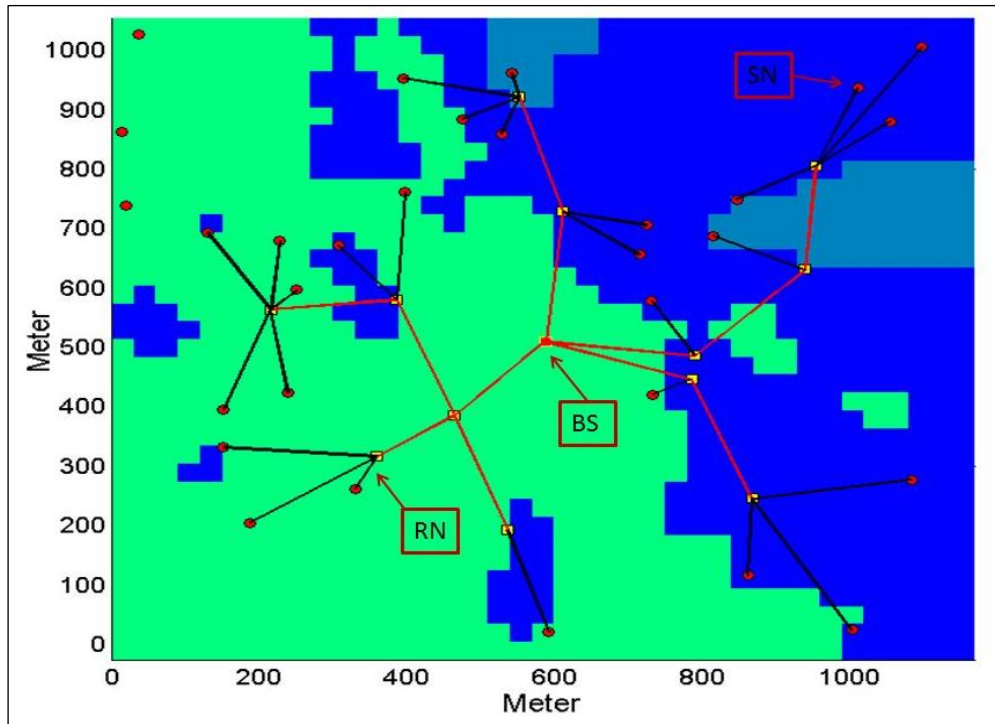
Figure 5.5: Optimization histories for RN=5

Figs. 5.6 and 5.7 show the corresponding results for $RN=12$. All the sensors are connected to the network for the free space, while there are still 3 unconnected sensors in the inhomogeneous field. To evaluate the necessary number of routers necessary or full connections of the sensors to WSNs, can perform optimizations changing the number of routers and random seeds.

The results are shown in Fig. 5.8, where can conclude are need at least 8 and 11 routers for the free space and inhomogeneous field. This number depends on the vegetation. The result can evaluate the necessary number of the routers for inhomogeneous field with arbitrary distribution.



(a) Free space



(b) Inhomogeneous field composed of forest, grassland and free space

Figure 5.6: Optimized topology for inhomogeneous RN=12

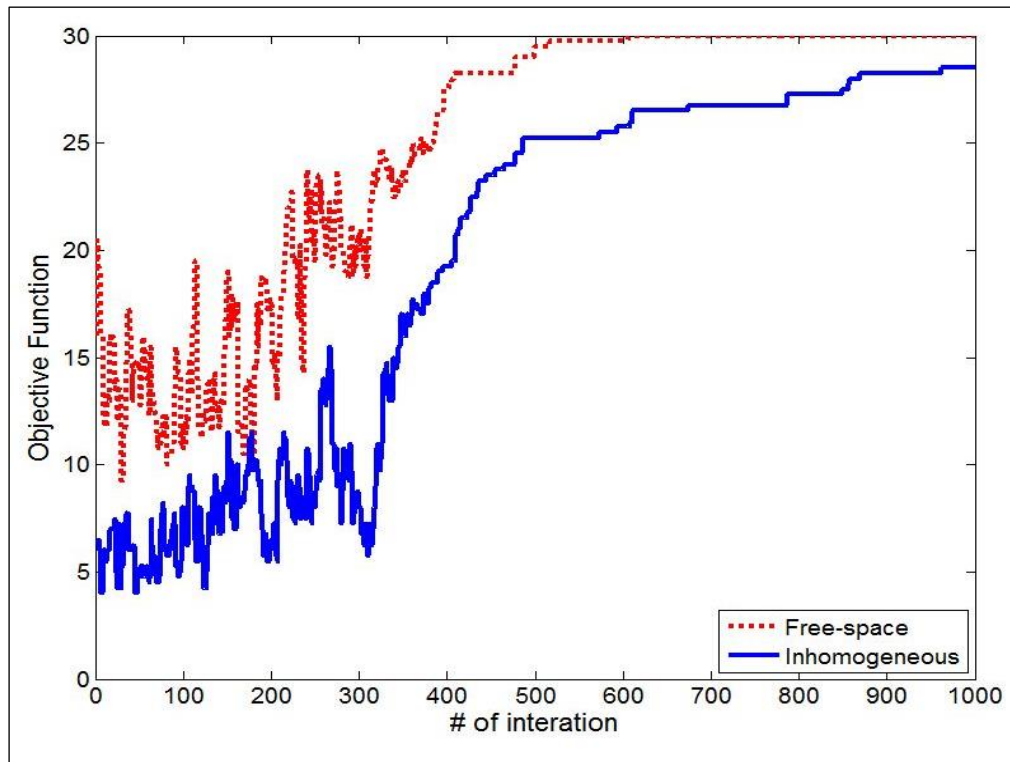
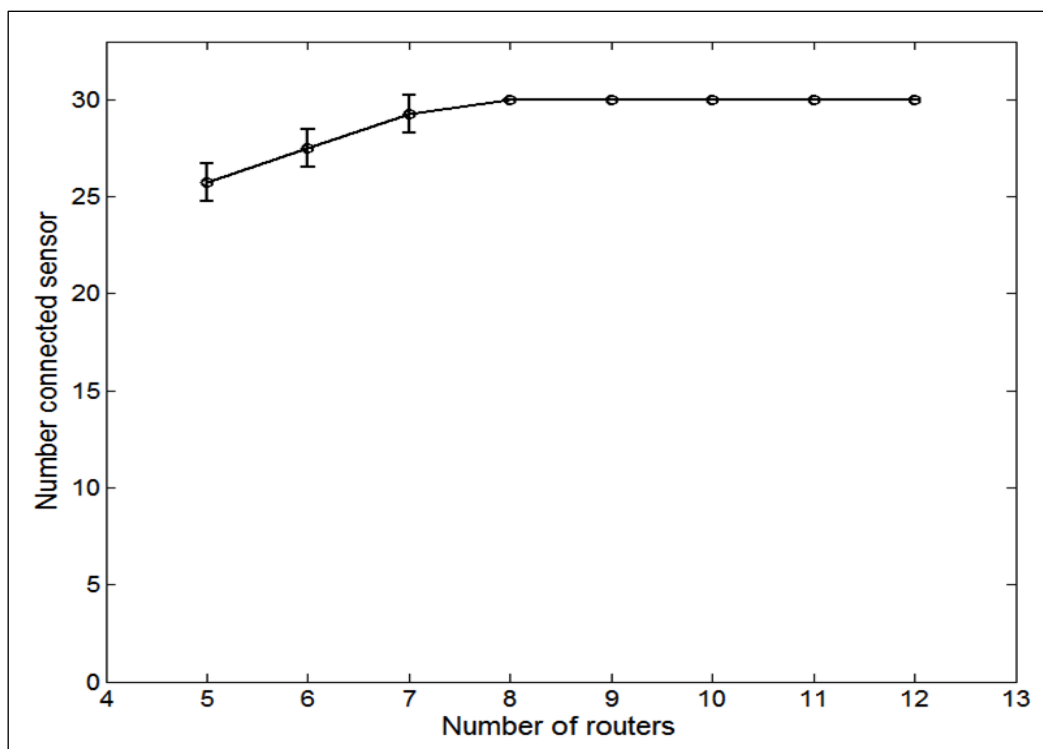
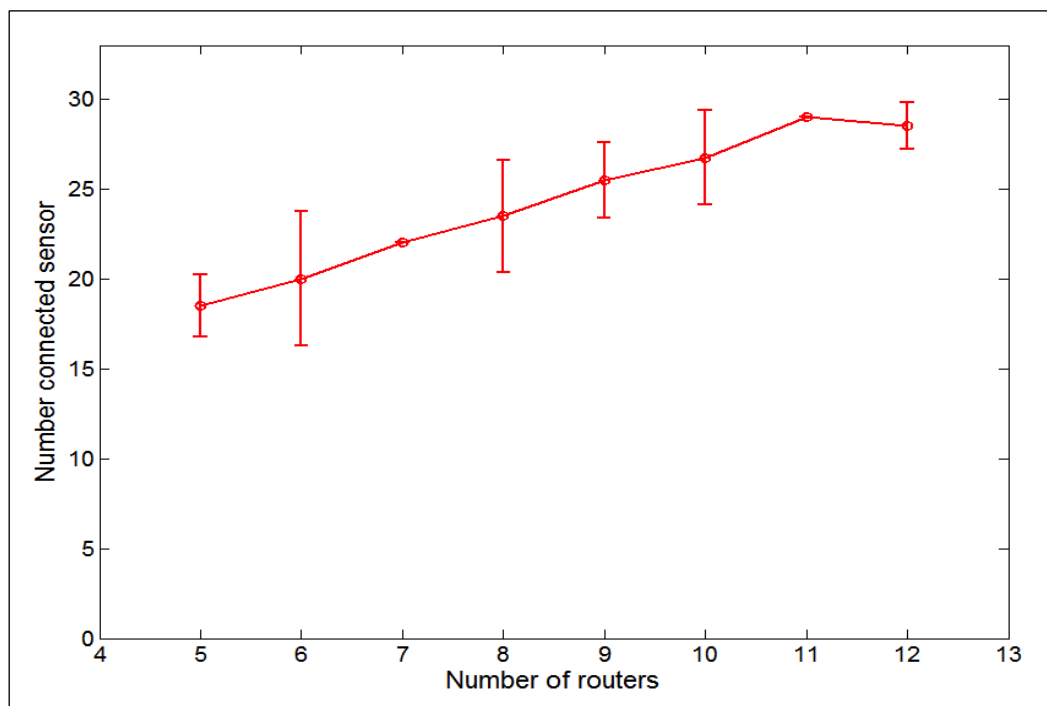


Figure 5.7: Optimization histories for RN=12



(a) Free space



(b) Inhomogeneous field composed of forest, grassland and free space

Figure 5.8: Number of connected sensors

5.2.3 Optimization of WSN for computed attenuation constants

In WSNs we consider a sensor network to detect forest fires. The sensor nodes are assumed to be randomly deployed in the forest. Moreover, it assumes that the sensor and router nodes have the communication distance R_0 in free space. It is clear that the number of the sensors which can communicate with the nearest parent node depends on the router deployment. The sensor is judged to be connected if the condition.

$$\frac{e^{-\int_0^R \alpha(r) dr}}{R} > \frac{1}{R_0}, \quad (5.1)$$

is satisfied, where R is the distance from the sensor to the nearest router including the base station. The value of $\alpha(r)$ is computed from (4.22)-(4.23).

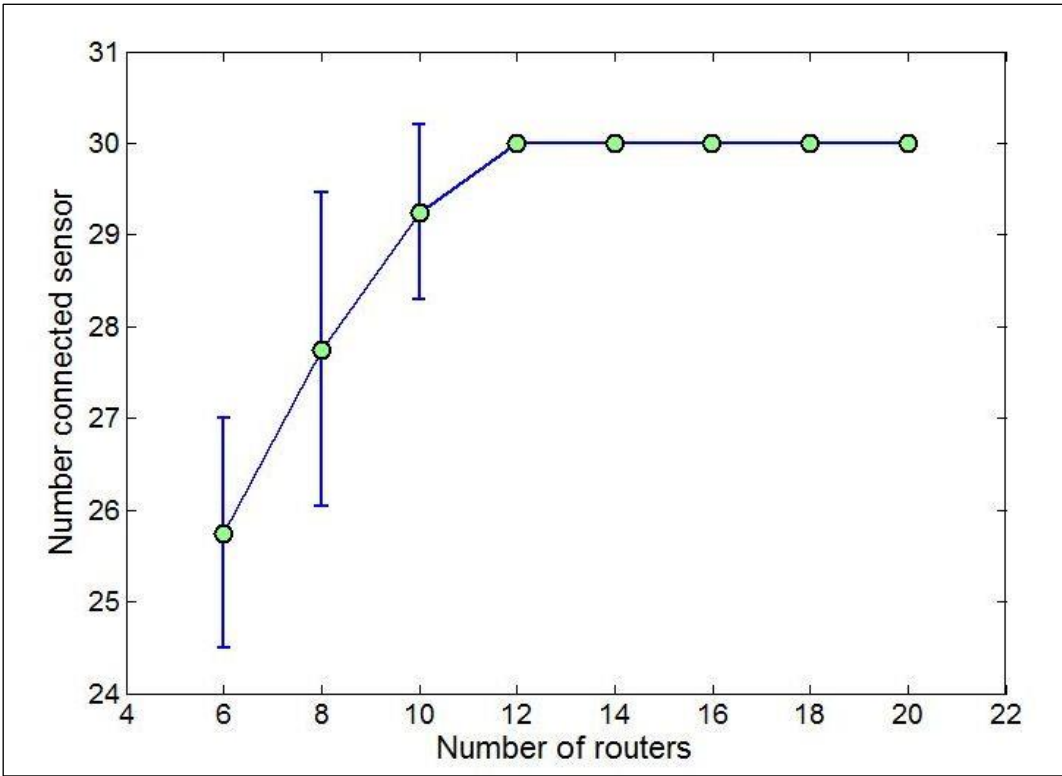
We optimize the router positions to maximize the number of connected sensors using the simulated annealing (SA) [77]. The optimization problem is defined by

$$N_c \rightarrow \max. \quad (5.2)$$

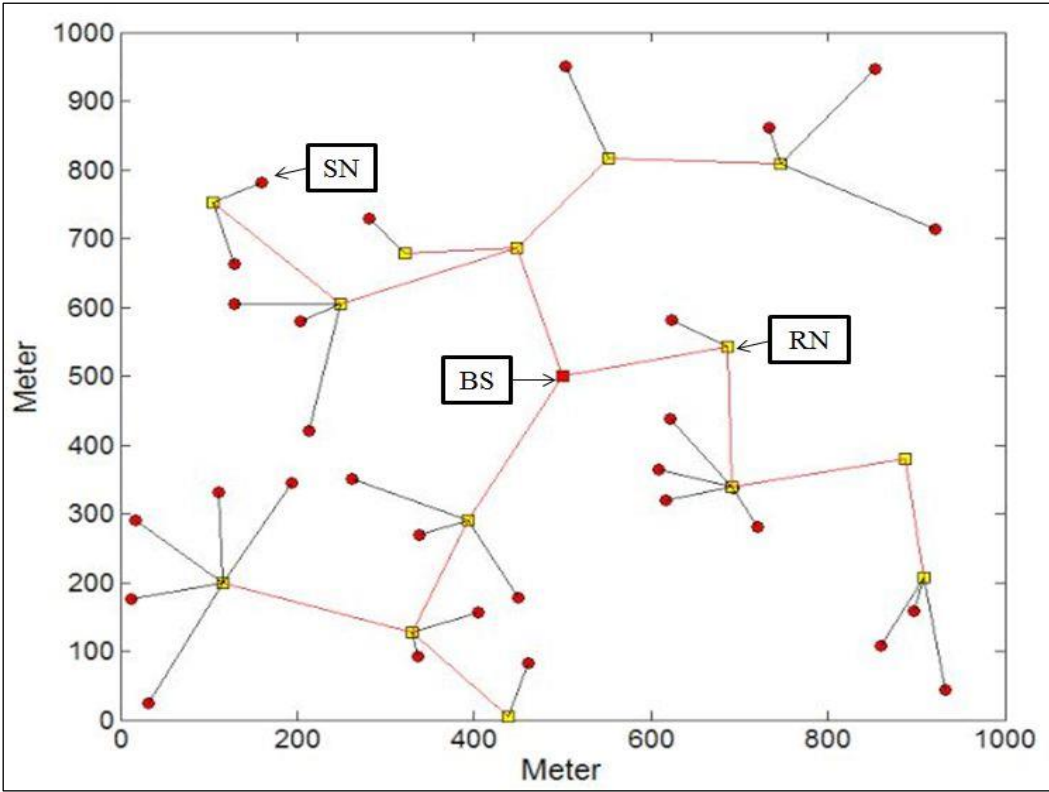
where N_c denotes the number of the connected sensors.

Figure 5.9 (a) shows the number of connected sensors deployed randomly in the sensing field with $\alpha = 3 \times 10^{-3}$, $R_0 = 500\text{m}$ where the router positions are optimized by simulated annealing. The number of sensors is set to 30. In WSN topology need 12 routers for full connection which are in good correspondence with the necessary router number read from Fig. 5.9. The optimized WSN topology and convergence history of simulated annealing are plotted in Fig. 5.9(b) and (c). Note that have much smaller number of connected sensors without the optimization as can be found from Fig. 5.9 (c).

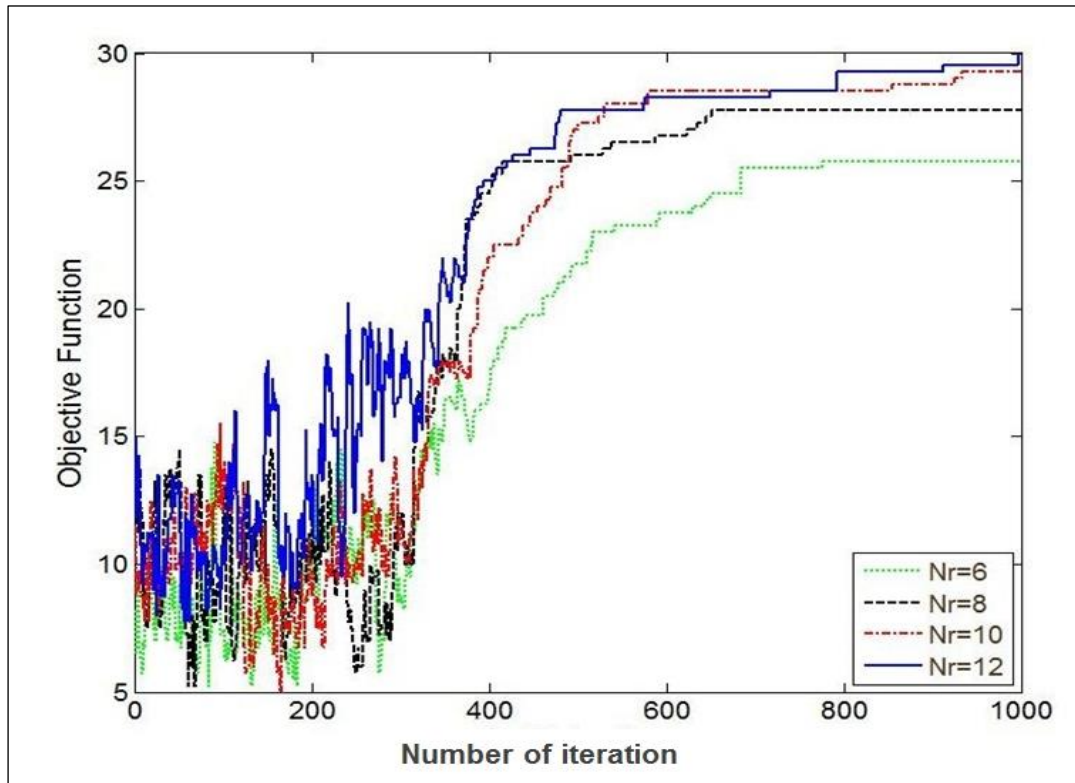
Now we consider the forest shown in Fig. 4.2. By assuming that the trees are infinite cylinder of the same radius, evaluate the values of the volume fraction from the basal area as $f = 2.86 \times 10^{-3}$, 1.87×10^{-3} , 1.84×10^{-3} for P1, P2 and P3, respectively.



(a) Number of connected sensors



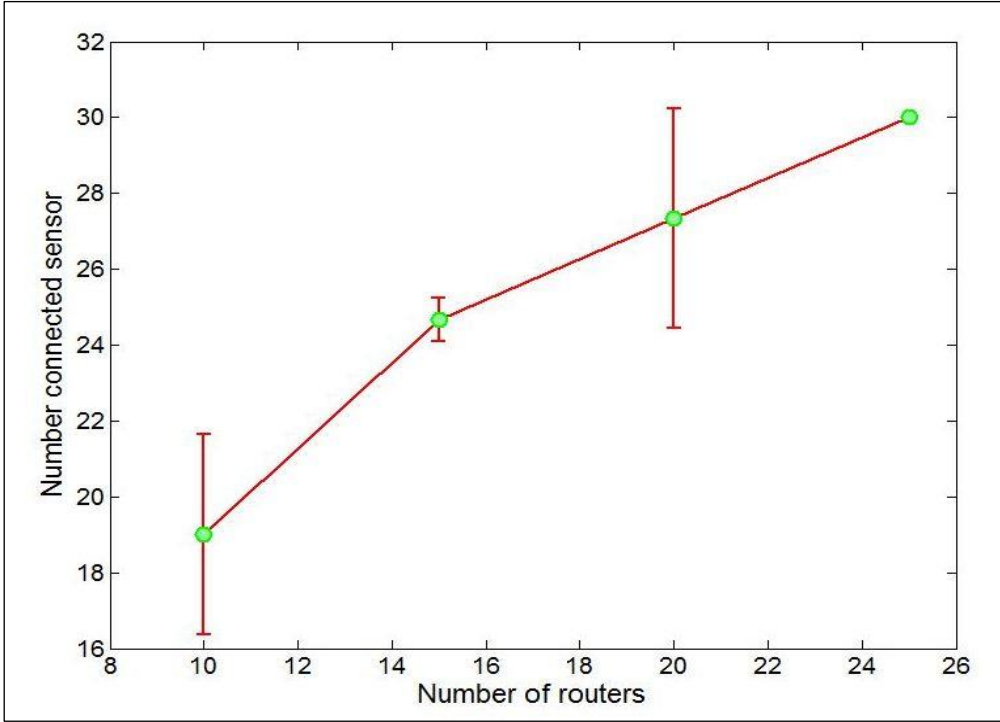
(b) WSN topology, RN=14



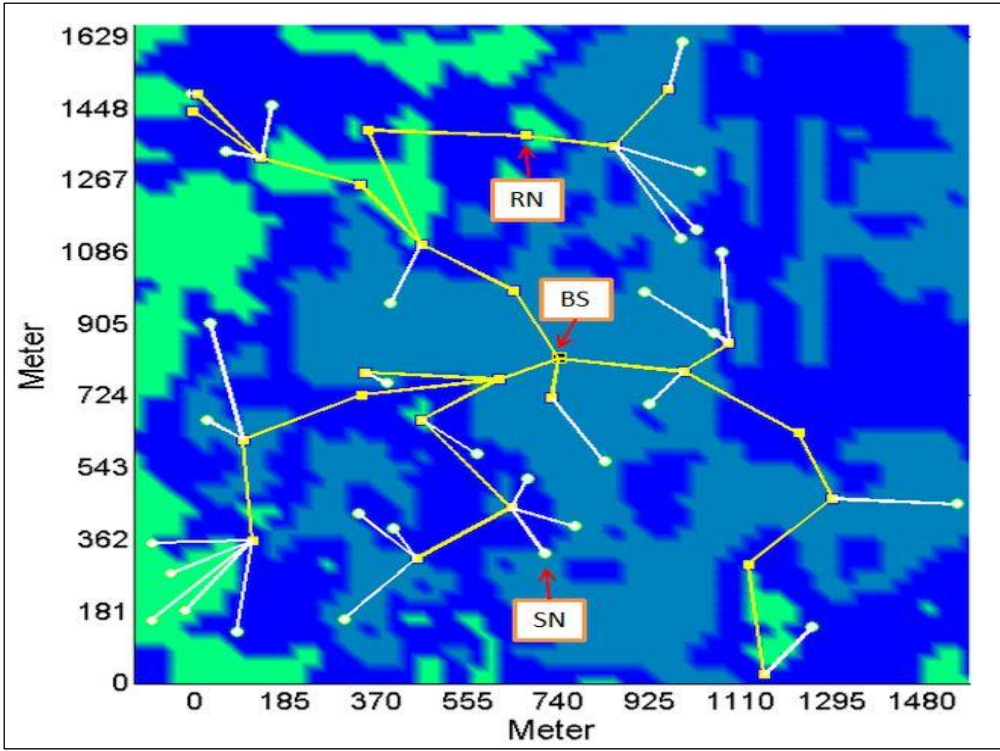
(c) Convergence history of SA

Figure 5.9: Optimization results for uniform sensing field, BS, RN, SN represent base station, router and sensor nodes, NR is number of routers $\alpha = 3 \times 10^{-3}$, $R_o = 500\text{m}$.

In this study, we optimize the router positions for WSN in the forest shown in Fig. 4.2. The wave polarization is chosen to be perpendicular to the trees. The value of attenuation constant depends on the position in this case. Figure 5.10 shows the resultant number of routers and WSN topology. The WSN topology can find that need 26 routers for full connection of the sensor nodes. We evaluate the attenuation constant α of forest based on the homogenization technique in which the basal area and complex permittivity of tree trunks are assumed to be given. The communication distance and number of routers necessary for full coverage of the sensing field have been obtained from α . It has been shown that electromagnetic waves with polarization perpendicular to tree trunks has longer propagation than those with parallel polarization. In this study can optimize the router deployment based on the evaluated value of α to maximize the connected number of sensors.



(a) Number of connected sensors



(b) WSN topology, NR=26

Figure 5.10: Optimization results for sensing field shown in Fig.4.2 $R_o=750m$.

5.3 Summary

The followings are concluded from the study mentioned in this section.

1. When the basal area and complex permittivity of tree trunks are given, we can evaluate the attenuation constant.
2. The communication distance and number of routers necessary for full coverage of the sensing field have been obtained from α .
3. It has been shown that electromagnetic waves with polarization perpendicular to tree trunks has longer propagation than those with parallel polarization.
4. We can optimize the router deployment based on the evaluated value of α to maximize the connected number of sensors.

Chapter 6 Optimization of WSN in irregular terrain

This chapter is devoted to discussion of optimization of WSN considering elevation differences in the sensing field. That is, when there are hills between a sensor and router, for example, they could not communicate with each other if the hill is higher than the Fresnel zone. For this reason, when we consider WSNs in irregular terrain, we have to consider the elevation differences. We optimize here the router deployment considering the elevation differences in irregular sensing fields.

6.1 Deployment of routers in elevation differences

In this study consider deployment sensor network in different elevation terrain. The router positions are optimized so that the total communication distance is minimized to maximize the lifetime of the sensor network. To consider the real geographical features of the target field, the elevation is considered in the optimization using digital elevation model data [86]. It is shown that can reduce the total communication distance as well as the number of disconnected sensors for both flat and irregular terrains using the present optimization method.

Wu et al. have optimized the sensor deployment on planar grid to maximize the detection probability within a given cost using GA[78]. They showed that their method outperforms a greedy sensor placement method. Bari et al. have optimized the data-gathering schedule for the relay nodes, which are equivalent to the routers, using GA[79]. Krishnamachari et al. have optimized the data flow among WSNs to maximize the total information routed to the sink node[80]. They showed that the maximum information which be extracted for a fixed amount of energy decreases as the fairness requirement is reduced. Zhao et al have discussed optimal deployment of high-powered relay nodes in static heterogeneous sensor networks [81]. The

genetic algorithm for integer planning is adopted to optimally deploy the relay nodes so as to obtain the optimal energy efficiency by minimizing the average path length. They consider the Manhattan distance in the optimization because the nodes are placed at the planar grid points.

In this study we optimize the router deployment for WSNs where the sensors are randomly distributed. The sensor networks take irregular elevation in the target field which affects communicability into account. The topology network also reduce the number of disconnected sensors which are outside the communication circles of the routers, which is included as a penalty in the objective function.

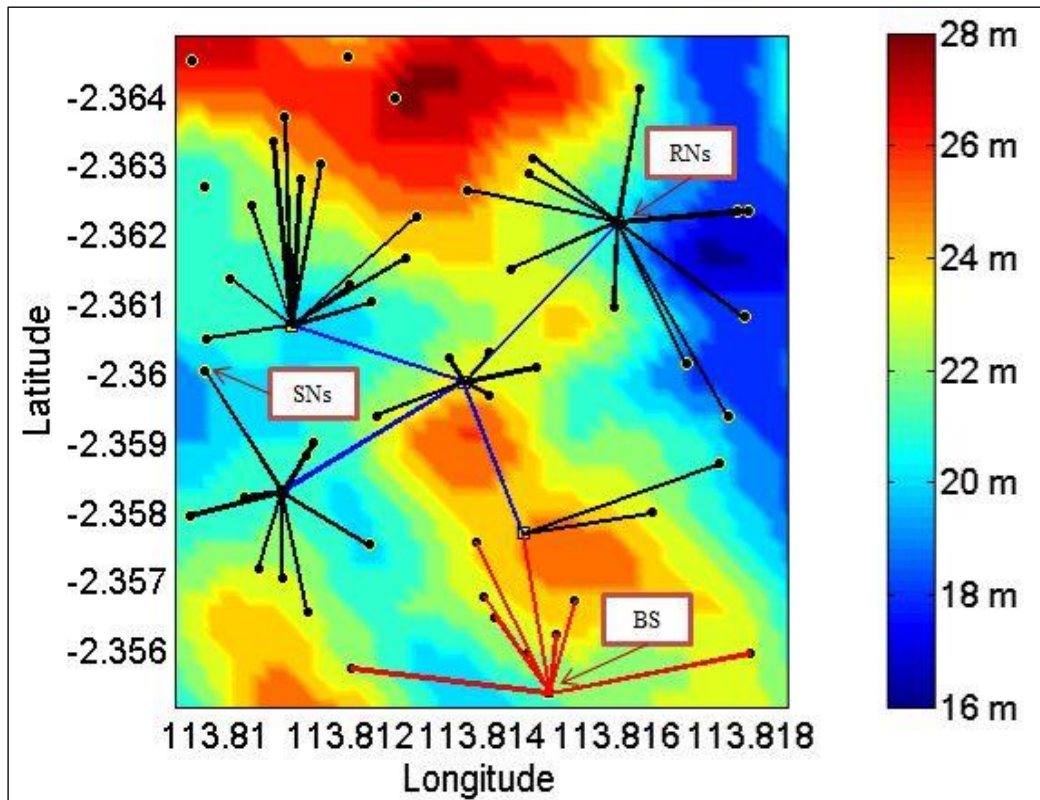


Figure 6.1: WSN in irregular terrain. The color represents elevation

6.2 Optimization problem

6.2.1 Problem definition

Let us consider the target field of $D_1 \times D_2 \text{ m}^2$. Figure 6.1 shows an example of WSN placed in a field with irregular elevation where $D_1 = D_2 = 1 \text{ km}$. The base station collects all the

sensed data from the routers and sensor nodes. It assumed that the base station has unlimited power for its operation. On the other hand, the routers and sensor nodes assumed to obtain power from the batteries mounted on them so that they are energy constrained. The sensor nodes detect environmental data such as temperature and humidity and send them to the nearest routers or base station. The routers collect data from the sensor nodes to send them to the base station. Due to the limitation in the power transmission of the routers and sensor nodes, they will use up the energy within the finite duration. It is necessary to maximize their lifetime because the replacement of the batteries is expensive especially when the sensors deployed in deep forest. The aim of this study is to find optimal deployment of the routers which maximizes the lifetime of WSN.

In this study we introduce a grid on the elevation contour map generated from the digital elevation model data [83]. According to the elevation, we utilize a linear interpolation based method to estimate the elevation values of points. It is assumed that N sensors are deployed at random location in the geographical map. The router and sensor node have communication radius R_r and R_s inside which they can communicate with other nodes. The optimization problem is defined by

$$F = \frac{1}{\sum_i^N d_i^2 + P} \rightarrow \max. \quad (6.1)$$

where d_i is the Euclid distance between i -th sensor node and its nearest parent node that is either router or base station. Moreover, P represents the penalty term which is defined by

$$P = nD_1D_2 \quad (6.2)$$

where n is the number of the disconnected sensor nodes. In the simulation, if there is a point whose elevation is above the line connected between two nodes then it is judged that the two nodes cannot communicate with each other (see Fig. 6.2). When we consider the flat terrain, there are no obstacles among the nodes. However, when we consider the sensor node in the irregular terrain, the network topology must be constructed taking the communicability into account. The present method can provide optimal network topology for both flat and irregular terrain.

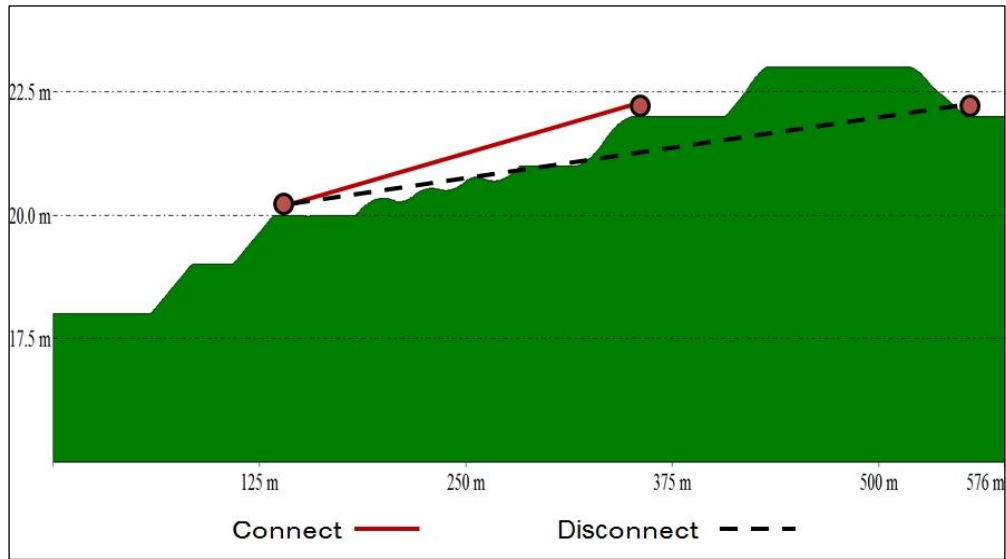


Figure 6.2: Test communicability of the sensor nodes

6.2.2 Real-Coded Genetic Algorithms (RGA)

In this study, we employ the real-coded genetic algorithms (RGA) for the optimization of router positions. The gene is composed of the coordinates of M routers, that is (x_1, x_2, \dots, x_M) , so that the degrees of freedom in the optimization is $2M$. The optimization parameters in RGA are summarized in Table 6.2. In particular, searching ability of RGA depends on crossover operation largely. In this work, the Blend crossover (BLX- α) is adoption for the crossover operator[82].

1. **Initial population.** Initial population is generated which has a given population size.
2. **Selection.** In this paper, we use roulette wheel selection which implements the proportional selection approach. In roulette wheel selection scheme which resembles survival of the fittest in nature, the chance to be selected for the reproduction of a chromosome is determined by its ratio of fitness value.
3. **Crossover.** The Blend-crossover process (BLX- α) generates two offspring from two individuals (parents). It randomly picks values that lie between two points that contain the two parents, but may extend equally on either side determined by a user specified parameter α .

4. **Mutation.** The coordinates \mathbf{x} of the routers are replaced by (pD_1, qD_2) where p and q are independent random numbers whose domain is $[0, 1]$.
5. **Optimal solution and terminal criterion.** The process of fitness computation, selection, crossover, and mutation is executed for a maximum number of iterations. To avoid possible elimination, a parent chromosome with the highest fitness is always copied into the next generation.

6.3 Optimization results

In this simulation we choose the peat forest in Central Kalimantan, Indonesia for a case study of the irregular terrain. The digital elevation model (DEM) of the location is obtained from the Shuttle Radar Topography Mission (SRTM) FTP site [86]. The elevation ranges from 16m to 28m. We also consider the flat terrain for comparison. In both cases, $D_1=D_2=1$ km.

In this model, the sensor and initial router nodes are placed randomly and the latter positions are optimized. In this simulation we use the same random seed for the optimizations.

Table 6.1: Simulation parameter

Parameter	Values
Location of base station	113.8185, -2.3610
Number of nodes	50
Number of routers, M	2, 3, 4, 5
Communication radius $R_s=R_r$	50 m, 100m, 200m, 400 m

Table 6.2: RGA parameter setting

Parameter	Values
Alpha	1.2
Population size	25
Crossover probability	100%
Mutation probability	20%
Number of generation	100

6.3.1 Optimization of WSN with small communication radius

In first simulation we consider the WSN which has communication radius $R_s=R_r=100\text{m}$. The number of routers, M , is set to five unless otherwise specified. Figures 6.3 and 6.4 show the optimized WSN deployment for flat and irregular terrain. In both case, there are many disconnected nodes because the maximum covered area $M\pi R_r^2$ is about 15% of the area of the target field D_1D_2 . It can be found that the communication paths are constructed so that there are no obstacles among them in Fig. 6.3.

Figure 6.5 shows the optimization history where we find that the fitness is monotonously improved. We also find in Fig.6.5 that the converged fitness value for the flat terrain is better than that for the irregular terrain. This is due to the fact that the communication paths in the irregular terrain must be formed avoiding the obstacles.

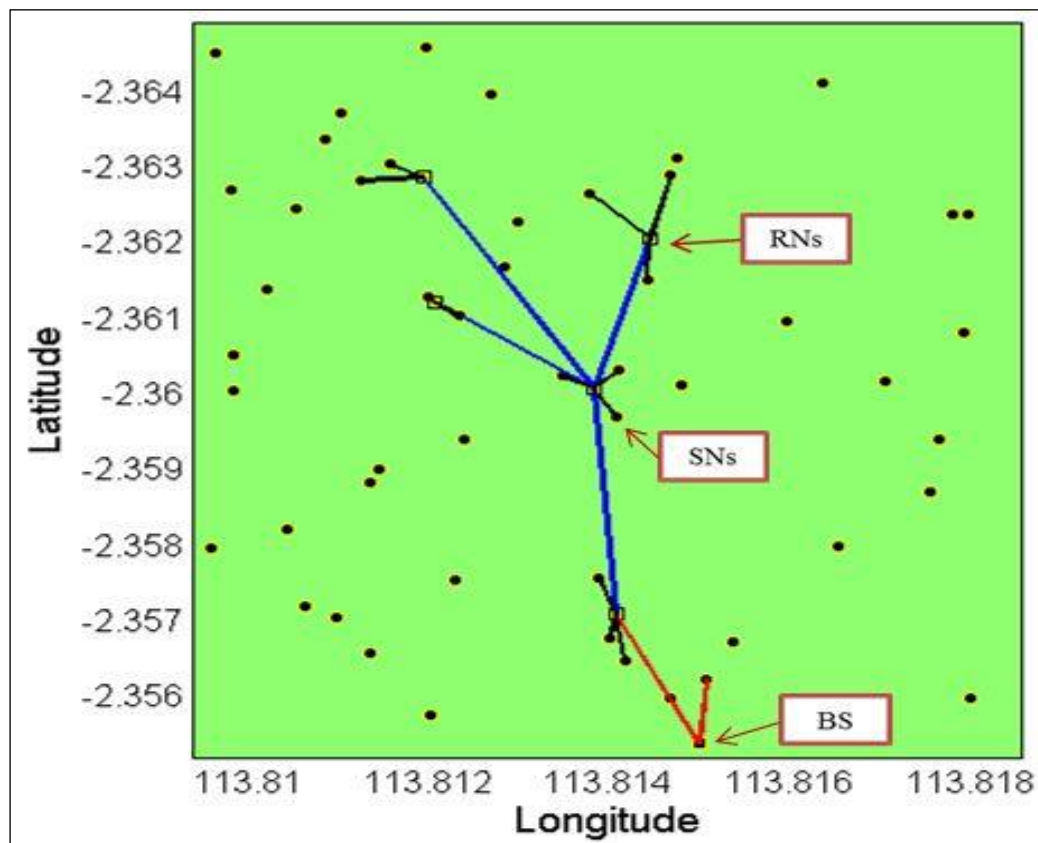


Figure 6.3: Optimized topology for flat terrain, $R_s=R_r=100\text{m}$, $M=5$

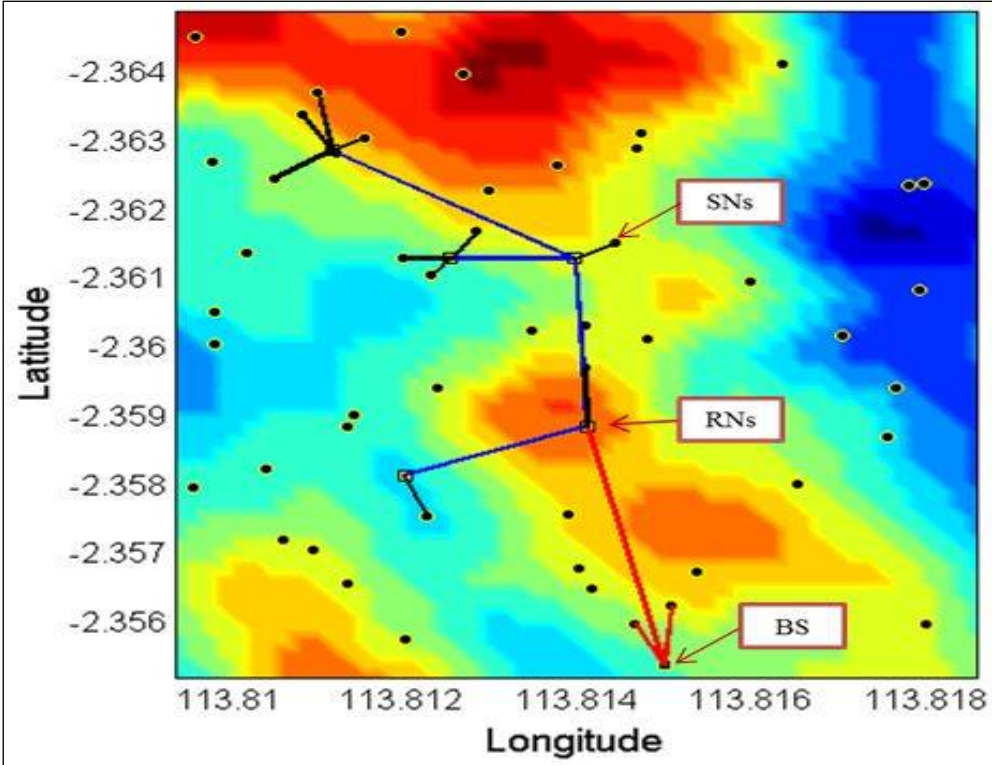


Figure 6.4: Optimized topology for irregular terrain, $R_s=R_r=100m$, $M=5$

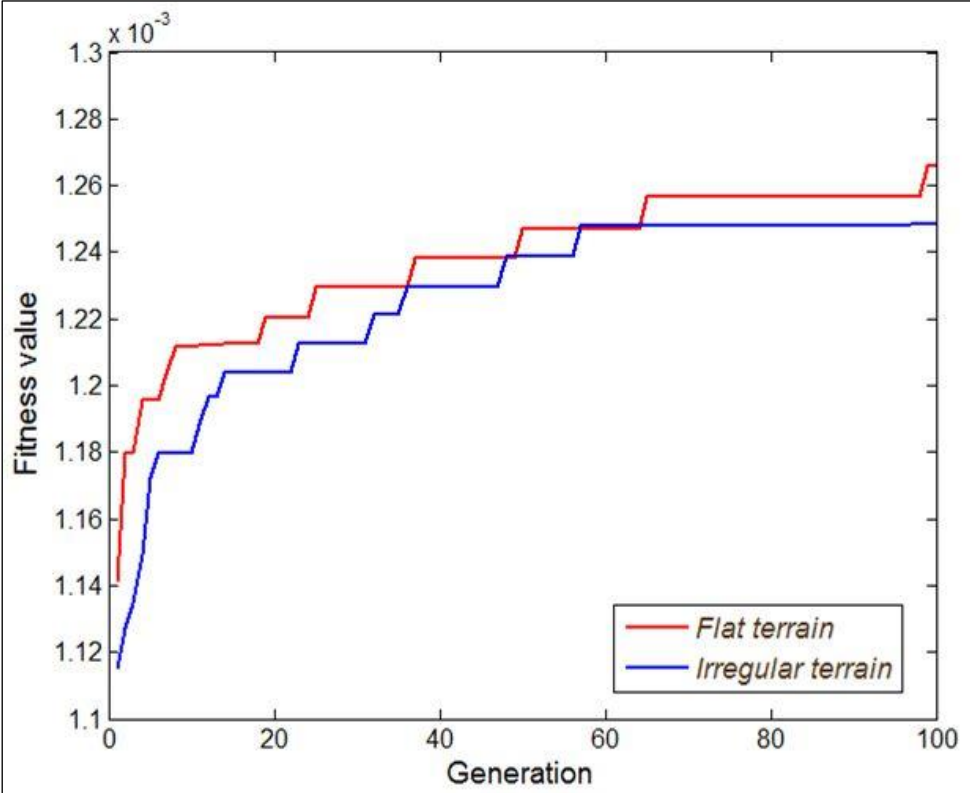


Figure 6.5: Optimization history when $R_s=R_r=100m$, $M=5$

6.3.2 Optimization of WSN with large communication radius

In next simulation the communication radius is increased up to 400m. Now the maximum covered area $M\pi R_r^2$ is about 250% of the target area. Figures Figure 6.6 and 6.7 show the optimized WSN topologies. There are no disconnected sensor nodes in both cases as expected. In Fig. 6.7 we find that there are no communication paths which go from valley to valley. Figure 6.8 shows the optimization history, which is similar to Fig. 6.5. The converged value of the fitness for the flat terrain is larger than that for the irregular terrain as expected.

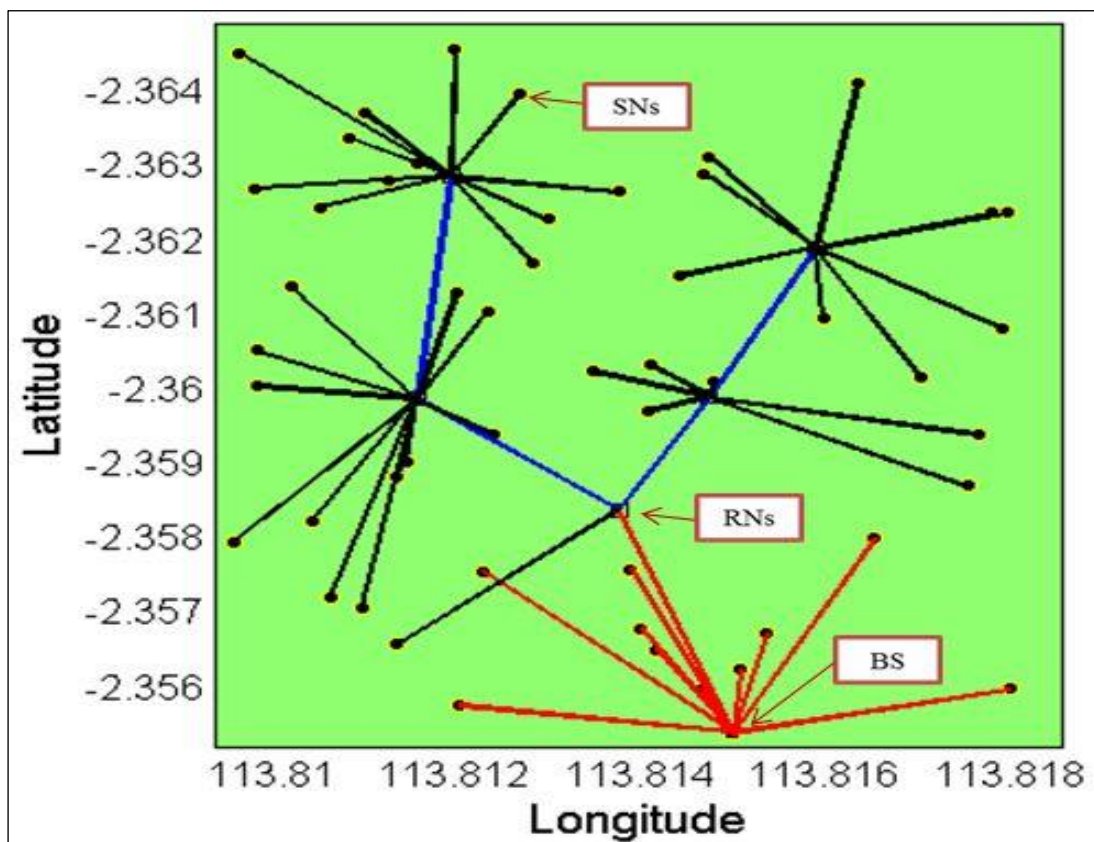


Figure 6.6 Optimized topology for flat terrain, $R_s=R_r=400\text{m}$, $M=5$

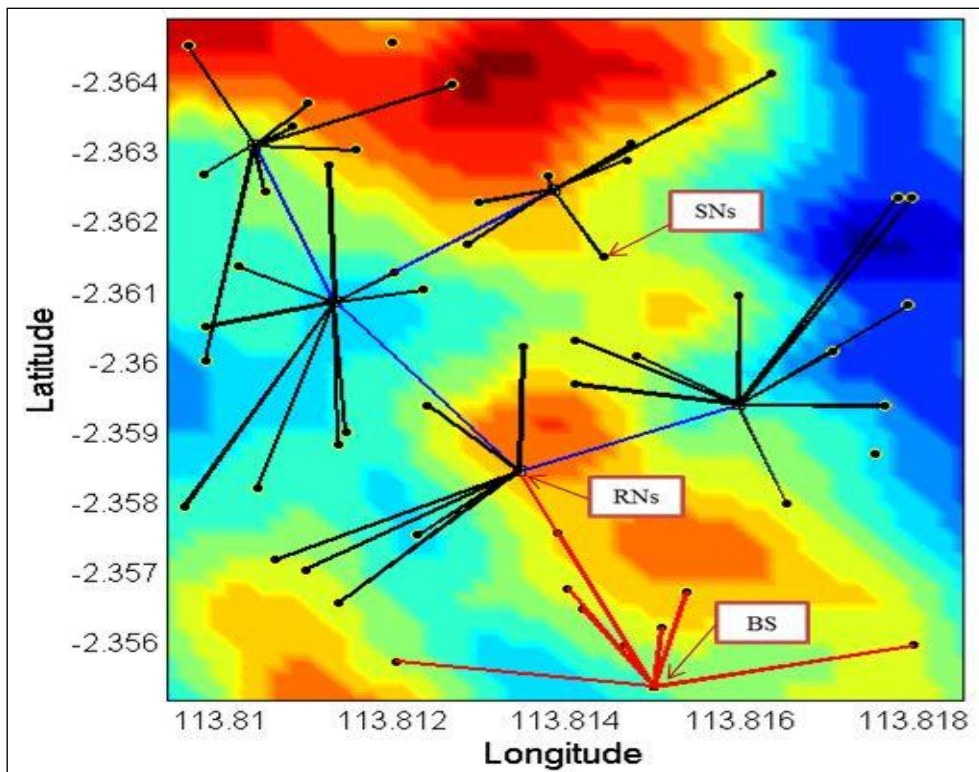


Figure 6.7: Optimized topology for irregular terrain, $R_s=R_r=400m$, $M=5$

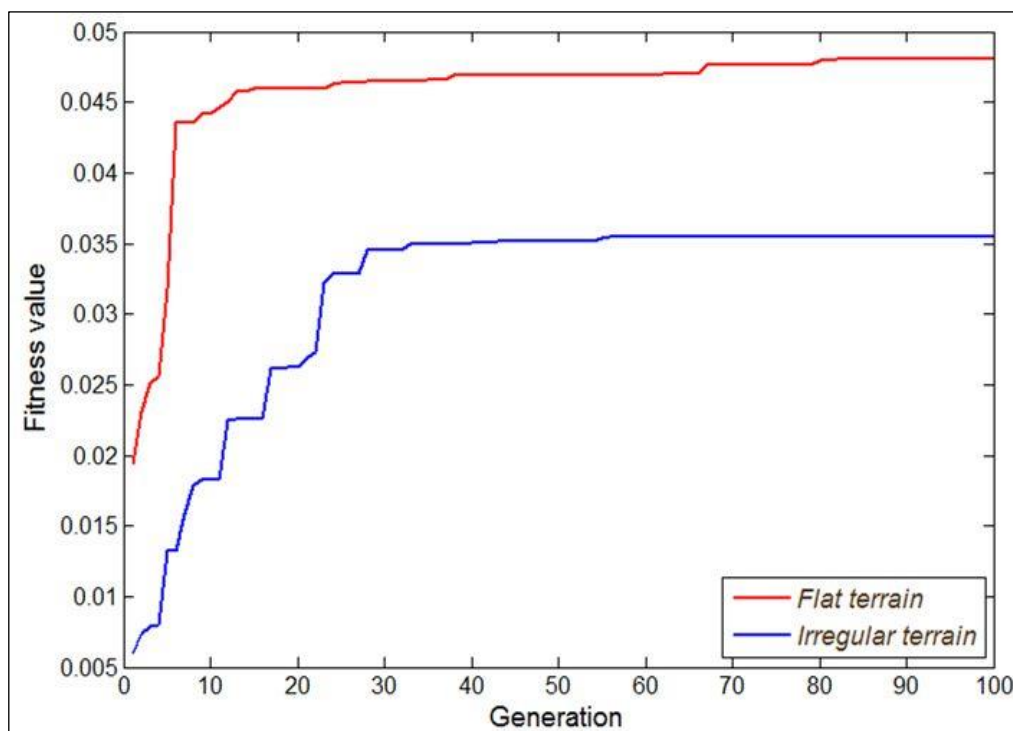


Figure 6.8: Optimization history when $R_s=R_r=400m$, $M=5$

6.3.3 Number of disconnected sensors

Next we consider dependence of the number of disconnected sensor nodes on the communication radius R_r and number of routers M . Figures 6.9 and 6.10 show changes of the numbers of disconnected sensor nodes in the WSNs which are optimized by the present method when R_r and number of routers M vary, while Figs. 6.11 and 6.12 shows them for non-optimized WSN where the routers are randomly deployed. We can find from these results that $M\pi R_r^2$ must be 150% and 250% at smallest for the flat and irregular terrains to have full connections of the sensors when WSNs are optimized. Note that the latter ratio depends on the terrain; we have to increase the ratio for highly irregular terrains. We can estimate the necessary ratio using the present method. On the other hand, we cannot have the full connections even when $M\pi R_r^2$ is about 250% for the non-optimized WSNs. It is concluded that the present optimization can reduce the total communication distance as well as number of disconnected sensor nodes.

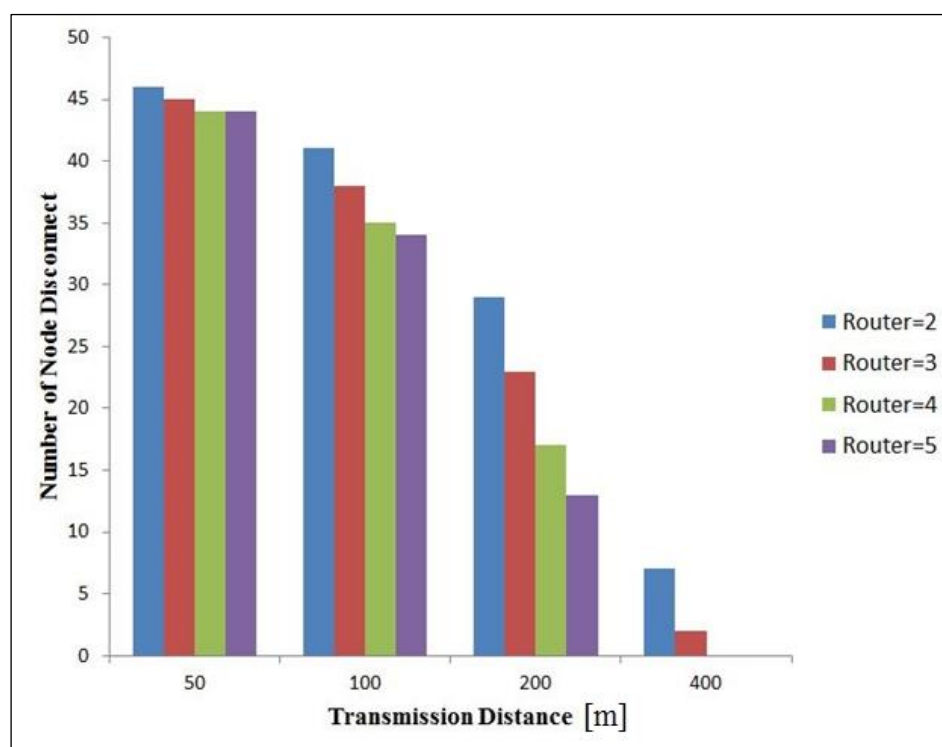


Figure 6.9: Number of disconnected sensor nodes for optimized WSN in flat terrain

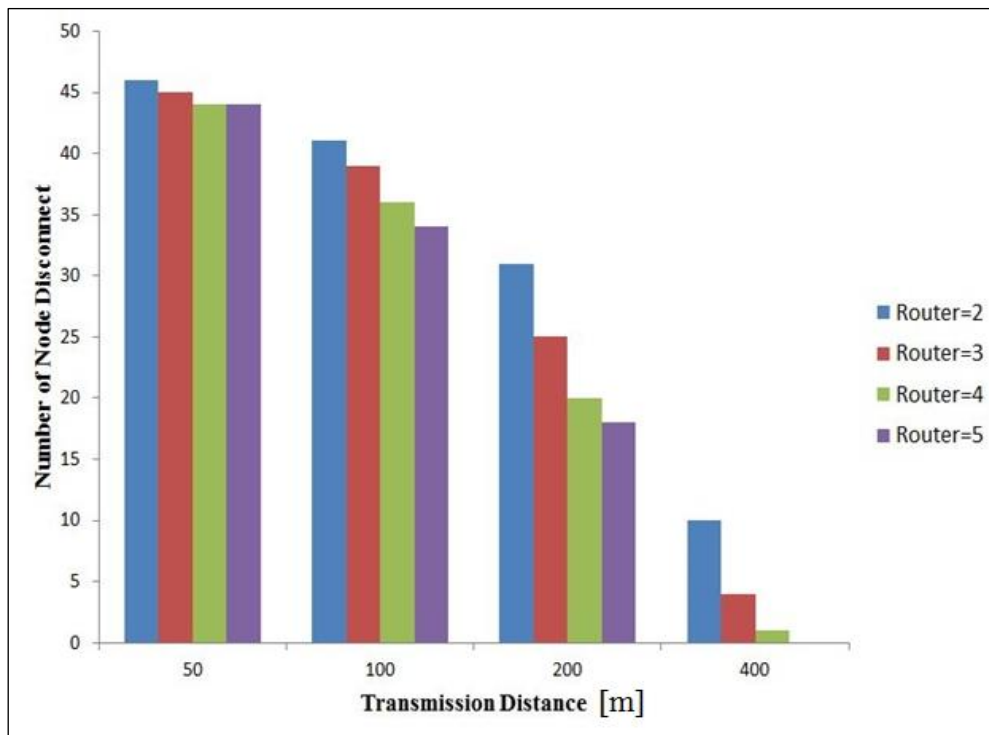


Figure 6.10 Number of disconnected sensor nodes for optimized WSN in irregular terrain

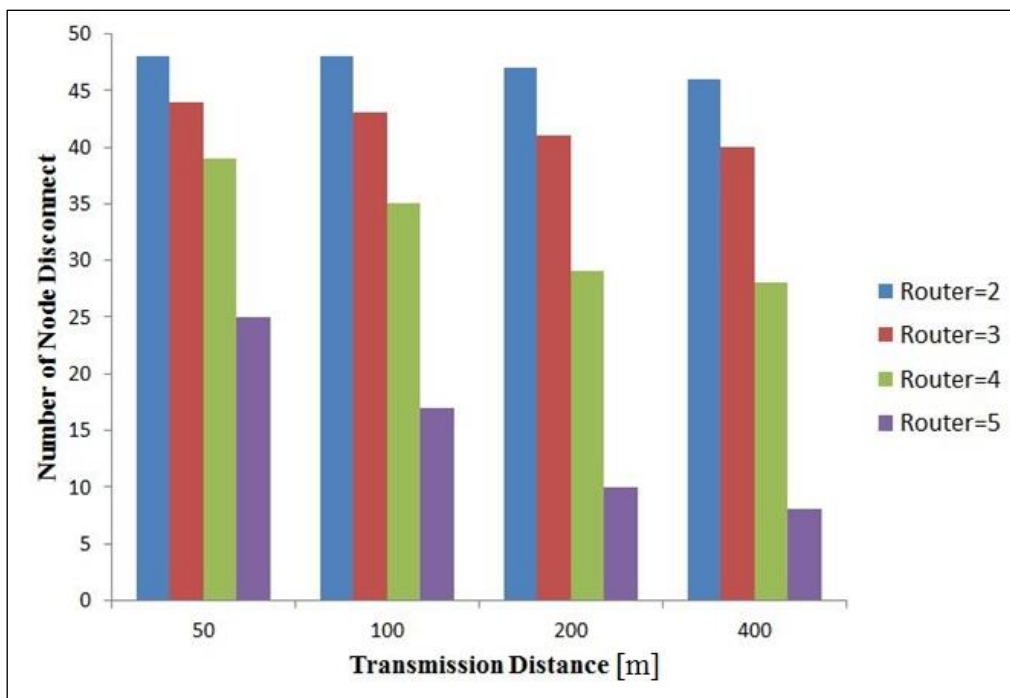


Figure 6.11: Number of disconnected sensor nodes for non-optimized WSN in flat terrain

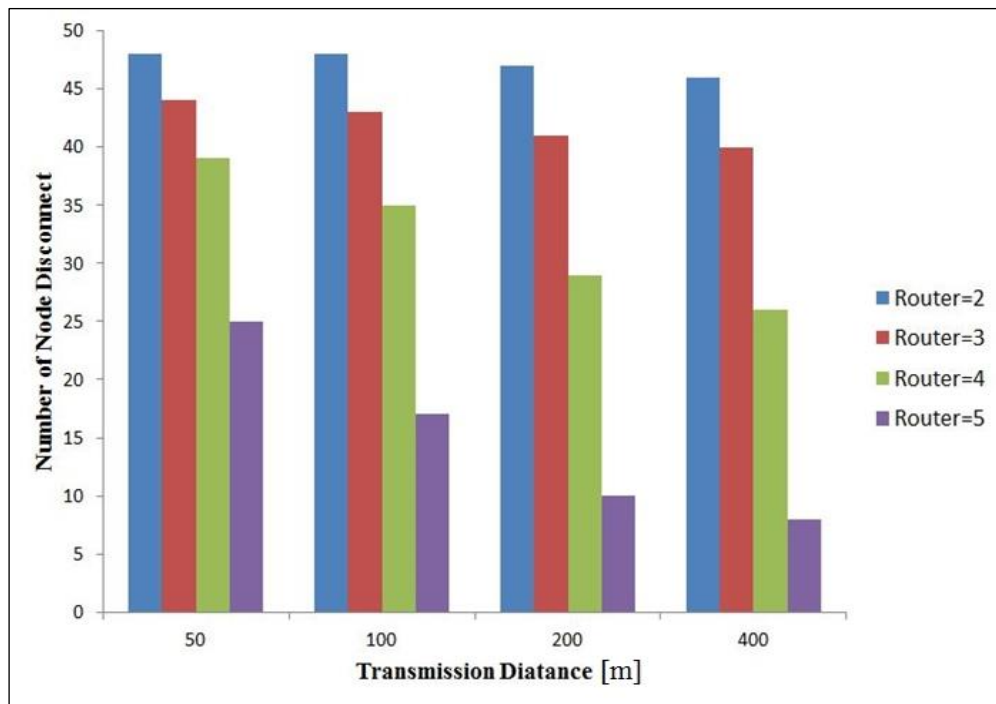


Figure 6.12: Number of disconnected sensor nodes for non-optimized WSN in irregular terrain

6.4 Summary

The followings are concluded from the study mentioned in this section.

1. By the optimization, we successfully obtain the WSN topology where the paths are set avoiding the obstacles between the sensor and router nodes.
2. The present optimization can reduce the total communication distance as well as number of disconnected sensor nodes.
3. The total communication distance for the irregular terrain is longer than that for the flat terrain. The maximum covered area $M\pi R_r^2$ must be 150% and 250% of the whole area for the flat terrain and the exemplified irregular terrain. The necessary ratio of $M\pi R_r^2$ to the whole target area can be computed by the present method.

Chapter 7 Conclusions

In this study, we have developed a new system for monitoring of wild fires. In this system, UAV is used to verify the data measured by the WSN. That is, when the abnormal temperature higher than 45 Celsius is measured by a sensor node in the WSN, the UAV flies to the heating spot for verification. If the image taken by the UAV includes real forest fire, the fire patrol is called. We also develop new method for optimization of WSN. In this method, we optimize the position of routers to maximize the number of connecting sensor nodes, and to minimize the total communication distance. In particular, we take the attenuation of EM waves due to vegetation and scattering due to differences in elevation into account.

In the first section, I have presented a background and purposes of my study for forest fires monitoring using wireless sensor networks and UAV in Central Kalimantan, Indonesia.

In the second section, I have reviewed the previous works on WSN and UAV. The originality of my work is use of UAV for verification of potential fires detected by sensor nodes in WSN. Moreover, I optimize the router positions in WSN whereas the sensor nodes are assumed to be deployed randomly. This optimization has not been discussed in other literature. Moreover, I take the attenuation and scattering of electromagnetic wave into account in the optimization. This is also new aspect of the present study.

In the third section, I have presented an effective technique to quickly detect and monitor peat forest based on WSN and UAV with focusing on their implementation and deployment in Central Kalimantan, Indonesia. Problems found in monitoring fires in peat lands are that satellites will not detect weak or small fires properly. Moreover, big fire will not easily be found in a haze or low visibility. Our WSN contains of miniature sensor nodes to collect environmental data such as temperature, relative humidity, light and barometric pressure, and to transmit more accurate information to fire patrol and remote monitor. We have verified WSN data collected from the ground sensing against the video surveillance data obtained from a UAV it is used for ground verification of satellite data in large peat forest areas.

In the fourth section, I have discussed propagation electromagnetic wave in the forest. We consider electromagnetic waves in inhomogeneous lossy dielectric media, which are governed by the Maxwell equations. In this study, the attenuation constant of waves is evaluated from complex permittivity and basal area of the forest using homogenization technique.

In the fifth section, I have discussed optimization of router deployment in WSN for wild fire detection. To determine optimal network topology of WSN, one has to know characteristics of electromagnetic wave propagation in forest. In this work, the attenuation constant of waves is evaluated from complex permittivity and basal area of the forest using homogenization technique. It is possible to evaluate the attenuation constant from the measured permittivity of tree trunks and the basal area. We have successfully optimized the router positions to maximize the number of connected sensor nodes. By using the present method, we can know the number of routers necessary for full connection of sensor nodes for given vegetation distribution.

In the sixth section, I have described optimization of router deployment based on genetic algorithm for energy-constrained wireless sensor networks which are used for wildfire monitoring. The router positions are optimized so that the total communication distance is minimized to maximize the lifetime of the sensor network. Moreover, we also maximize the number of the connected sensor nodes. To consider the real geographical features of the target field, the difference in elevation is considered in the optimization using digital elevation model data. It is shown that we can reduce the total communication distance as well as the number of disconnected sensors for both flat and irregular terrains using the present optimization method.

References

- [1] S. E. Page, F. Siegert, J. O. Rieley, H. V Boehm, A. Jaya, and S. Limin, "The amount of carbon released from peat and forest fires in Indonesia during 1997," *Nature*, vol. 420, pp. 61–65, 2002.
- [2] A. Usup, Y. Hashimoto, H. Takahashi, and H. Hayasaka, "Combustion and thermal characteristics of peat fire in tropical peatland in Central Kalimantan , Indonesia," *Tropics*, vol. 14, pp. 1–20, 2004.
- [3] T. Hirano, J. Jauhainen, T. Inoue, and H. Takahashi, "Controls on the Carbon Balance of Tropical Peatlands," *Ecosystems*, vol. 12, no. 6, pp. 873–887, 2008.
- [4] S. Limin, H. Takahashi, A. Usup, and H. Hayasaka, "Impacts of haze in 2002 on social activity and human health in Palangka Raya," *Tropics*, vol. 16, no. 3, pp. 275–282, 2002.
- [5] H. Segah, H. Tani, and T. Hirano, "Detection of fire impact and vegetation recovery over tropical peat swamp forest by satellite data and ground-based NDVI instrument," *Int. J. Remote Sens.*, vol. 31, no. 20, pp. 5297–5314, 2010.
- [6] N. Yulianti, H. Hayasaka, and A. Sepriando, "Recent Trends of Fire Occurrence in Sumatra (Analysis Using MODIS Hotspot Data): A Comparison with Fire Occurrence in Kalimantan," *Open Journal Forestry.*, vol. 3, no. 4, pp. 129–137, 2013.
- [7] R. Teguh, T. Honma, A. Usop, H. Shin, and H. Igarashi, "Detection and Verification of Potential Peat Fire Using Wireless Sensor Network and UAV," *CITEE*, pp. 6–10, 2012.
- [8] M. Younis and K. Akkaya, "Strategies and techniques for node placement in wireless sensor networks: A survey," *Ad Hoc Networks*, vol. 6, no. 4, pp. 621–655, 2008.
- [9] S. N. Vecherin, D. K. Wilson, and C. L. Pettit, "Optimal sensor placement with signal propagation effects and inhomogeneous coverage preferences," *International Journal Sensor Networks*, vol. 9, no. 2, p. 107, 2011.
- [10] P. Cheng, C. Chuah, and X. Liu, "Energy-aware node placement in wireless sensor networks," *IEEE Global Telecommunication.*, vol. 5, pp. 3210–3214, 2004.
- [11] A. Hussain, P. Khan, and K. S. Kwak, "WSN Research Activities for Military Application," *ICACT*, pp. 271–274, 2009.
- [12] E. Cayirci, H. Tezcan, Y. Dogan, and V. Coskun, "Wireless sensor networks for underwater surveillance systems," *Ad Hoc Networks*, vol. 4, pp. 431–446, 2006.

References

- [13] S. Simoni, S. Padoan, D. F. Nadeau, M. Diebold, A. Porporato, G. Barrenetxea, F. Ingelrest, M. Vetterli, and M. B. Parlange, “Hydrologic response of an alpine watershed: Application of a meteorological wireless sensor network to understand streamflow generation,” *Water Resource Research.*, vol. 47, no. 10, pp. 1–16, 2011.
- [14] I. Yoon, D. K. Noh, D. Lee, R. Teguh, T. Honma, and H. Shin, “Reliable Wildfire Monitoring with Sparsely Deployed Wireless Sensor Networks,” *IEEE 26th Int. Advanced. Information Network Application.*, pp. 460–466, 2012.
- [15] K. Bouabdellah, H. Noureddine, and S. Larbi, “Using Wireless Sensor Networks for Reliable Forest Fires Detection,” *Procedia Computer Science.*, vol. 19, pp. 794–801, 2013.
- [16] Q. Zhang, J. Li, J. Rong, X. Weiheng, and H. Jinping, “Application of WSN in precision forestry,” *Electron Measurement Instruments*, pp. 320 – 323, 2011.
- [17] S. M. Abd El-kader and B. M. Mohammad El-Basioni, “Precision farming solution in Egypt using the wireless sensor network technology,” *Egypt. Informatics Journal*, vol. 14, no. 3, pp. 221–233, 2013.
- [18] J. a. López Riquelme, F. Soto, J. Suardíaz, P. Sánchez, a. Iborra, and J. a. Vera, “Wireless Sensor Networks for precision horticulture in Southern Spain,” *Computer Electronic. Agriculture.*, vol. 68, no. 1, pp. 25–35, 2009.
- [19] X. Yu, P. Wu, W. Han, and Z. Zhang, “A survey on wireless sensor network infrastructure for agriculture,” *Computer Standar Interfaces*, vol. 35, no. 1, pp. 59–64, 2013.
- [20] H. Alemdar and C. Ersoy, “Wireless sensor networks for healthcare: A survey,” *Computer Networks*, vol. 54, no. 15, pp. 2688–2710, 2010.
- [21] A. Milenković, C. Otto, and E. Jovanov, “Wireless sensor networks for personal health monitoring: Issues and an implementation,” *Computer Communication*, vol. 29, no. 13–14, pp. 2521–2533, 2006.
- [22] M. Castillo-Effen, D. H. Quintela, R. Jordan, W. Westhoff, and W. Moreno, “Wireless sensor networks for flash-flood alerting,” *IEEE Int. Caracas Conf. Devices, Circuits System*, pp. 142–146, 2004.
- [23] M. V. Ramesh, “Real-Time Wireless Sensor Network for Landslide Detection,” *International Conference Sensor Technology Application.*, pp. 405–409, 2009.
- [24] G. Wemer-allen, J. Johnson, M. Ruid, J. Lees, and M. Welsh, “Monitoring Volcanic Eruptions with a Wireless Sensor Network,” *Wireless Sensor Networks*, pp. 108 – 120, 2005.

- [25] X. Niu, C. Wei, and L. Wang, "The Design of a Wireless Sensor Network for Seismic-Observation-Environment Surveillance," *LNCS 6843, Springer*, pp. 157–167, 2011.
- [26] O. Younis, M. Krunz, and S. Ramasubramanian, "Node Clustering in Wireless Sensor Networks: Recent Developments and Deployment Challenges," *Network, IEEE*, vol. 20, no. 3, pp. 20–25, 2006.
- [27] E. L. Lloyd and G. Xue, "Relay Node Placement in Wireless Sensor Networks," *IEEE Trans. Comput.*, vol. 56, no. 1, pp. 134–138, 2007.
- [28] W. R. Heinzelman, A. Chandrakasan, and H. Balakrishnan, "Energy-Efficient Communication Protocol for Wireless Microsensor Networks," *System Science.*, pp. 1–10, 2000.
- [29] A. A. Abbasi and M. Younis, "A survey on clustering algorithms for wireless sensor networks," *Computer Communication.*, vol. 30, no. 14–15, pp. 2826–2841, 2007.
- [30] O. Younis and S. Fahmy, "HEED : A Hybrid , Energy-Efficient , Distributed Clustering Approach for Ad-hoc Sensor Networks," *Mobile Computation.*, vol. 3, no. 4, pp. 366 – 379, 2004.
- [31] C. Chong and S. P. Kumar, "Sensor Networks : Evolution, Opportunities , and Challenges," *Proc. IEEE*, vol. 91, no. 8, pp. 1247 – 1256, 2003.
- [32] I. F. Akyildiz, W. Su, Y. Sankarasubramaniam, and E. Cayirci, "Wireless sensor networks: a survey," *Computer Networks*, vol. 38, no. 4, pp. 393–422, 2002.
- [33] R. Teguh, R. Murakami, and H. Igarashi, "Optimization of Router Deployment for Sensor Networks Using Genetic Algorithm," *ICAISC Part I*, pp. 468–479, 2014.
- [34] M. Haghpanahi, M. Kalantari, and M. Shayman, "Topology control in large-scale wireless sensor networks: Between information source and sink," *Ad Hoc Networks*, vol. 11, no. 3, pp. 975–990, 2013.
- [35] H. Wang, N. Agoulmine, M. Ma, and Y. Jin, "Network lifetime optimization in wireless sensor networks," *IEEE Journal Selected. Areas Communication.*, vol. 28, no. 7, pp. 1127–1137, 2010.
- [36] X. Zhang and Z. Da Wu, "The balance of routing energy consumption in wireless sensor networks," *J. Parallel Distrib. Comput.*, vol. 71, no. 7, pp. 1024–1033, 2011.
- [37] K. Akkaya, F. Senel, and B. McLaughlan, "Clustering of wireless sensor and actor networks based on sensor distribution and connectivity," *Journal Parallel Distribution Computer*, vol. 69, no. 6, pp. 573–587, 2009.

References

- [38] S. Bandyopadhyay and E. J. Coyle, “An Energy Efficient Hierarchical Clustering Algorithm for Wireless Sensor Networks,” *INFOCOM*, vol. 3, pp. 1713 – 1723, 2003.
- [39] M. Ye, C. Lil, G. Chenl, and J. Wu, “EECS : An Energy Efficient Clustering Scheme in Wireless Sensor Networks,” *IPCCC*, pp. 535 – 540, 2005.
- [40] L. Qing, Q. Zhu, and M. Wang, “Design of a distributed energy-efficient clustering algorithm for heterogeneous wireless sensor networks,” *Computer Communication.*, vol. 29, no. 12, pp. 2230–2237, 2006.
- [41] J. Yick, B. Mukherjee, and D. Ghosal, “Wireless sensor network survey,” *Computer Networks*, vol. 52, no. 12, pp. 2292–2330, 2008.
- [42] P. Baronti, P. Pillai, V. W. C. Chook, S. Chessa, A. Gotta, and Y. F. Hu, “Wireless sensor networks: A survey on the state of the art and the 802.15.4 and ZigBee standards,” *Computer Communication.*, vol. 30, no. 7, pp. 1655–1695, 2007.
- [43] L. Ruiz-Garcia, P. Barreiro, and J. I. Robla, “Performance of ZigBee-Based wireless sensor nodes for real-time monitoring of fruit logistics,” *Journal Food Engineering.*, vol. 87, no. 3, pp. 405–415, Aug. 2008.
- [44] T. Rama Rao, D. Balachander, a. Nanda Kiran, and S. Oscar, “RF propagation measurements in forest & plantation environments for Wireless Sensor Networks,” *2012 International Conference Recent Trends Information Technology.*, pp. 308–313, 2012.
- [45] G. Anastasi and M. Conti, “Reliability and energy efficiency in multi-hop IEEE 802.15.4/ZigBee wireless sensor networks,” *ISCC*, pp. 336–341, 2010.
- [46] V. Raghunathan, A. Kansal, J. Hsu, J. Friedman, and M. Srivastava, “Design Considerations for Solar Energy Harvesting Wireless Embedded Systems,” *IPSN*, pp. 457 – 462, 2005.
- [47] S. Roundy, D. Steingart, L. Frechette, P. Wright, and J. Rabaey, “Power Sources for Wireless Sensor Networks,” *LNCS 2920, Springer*, pp. 1–17, 2004.
- [48] A. Boukerche, B. Turgut, N. Aydin, M. Z. Ahmad, L. Bölöni, and D. Turgut, “Routing protocols in ad hoc networks: A survey,” *Computer Networks*, vol. 55, no. 13, pp. 3032–3080, 2011.
- [49] E. Alotaibi and B. Mukherjee, “A survey on routing algorithms for wireless Ad-Hoc and mesh networks,” *Computer Networks*, vol. 56, no. 2, pp. 940–965, 2012.
- [50] A. Somov, “Wildfire safety with wireless sensor networks,” *ICST Trans. Ambient System.*, vol. 11, no. 10–12, pp. 1–11, 2011.
- [51] A. Restas, “Forest Fire Management Supporting by UAV Based Air Reconnaissance Results of Szendro Fire Department , Hungary,” *ISEIMA,IEEE*, pp. 73–77, 2006.

- [52] A. Ollero, J. R. Artíz-de-Dios, and L. Merino, "Unmanned aerial vehicles as tools for forest-fire fighting," *For. fire Res.*, Nov. 2006.
- [53] C. Suh, J. Joung, and Y. Ko, "New RF Models of the TinyOS Simulator," *WCNC, IEEE*, pp. 2238–2242, 2007.
- [54] S. Abbate, M. Avvenuti, D. Cesarini, and A. Vecchio, "Estimation of Energy Consumption for TinyOS 2.x-Based Applications," *Procedia Computer Science.*, vol. 10, pp. 1166–1171, 2012.
- [55] F. Cuomo, E. Cipollone, and A. Abbagnale, "Performance analysis of IEEE 802.15.4 wireless sensor networks: An insight into the topology formation process," *Computer Networks*, vol. 53, no. 18, pp. 3057–3075, 2009.
- [56] J. S. Seybold, *Introduction to RF Propagation*. John Wiley & Sons, Inc., 2005.
- [57] D. W. Casbeer, R. W. Beard, R. K. Mehra, and T. W. McLain, "Forest fire monitoring with multiple small UAVs," *American Control Conference. 2005.*, pp. 3530–3535, 2005.
- [58] M. Luis, J. Wiklund, F. Caballero, A. Moe, J. ramiro martinez-de Dios, P. Forssen, K. Nordberg, and A. Ollero, "Vision-Based Multi-UAV Position Estimation," *Robot. Autom. Magazine.*, pp. 53–62, 2006.
- [59] T. Arnold, M. De Biasio, A. Fritz, and R. Leitner, "UAV-based multispectral environmental monitoring," *IEEE Sensors*, pp. 995–998, 2010.
- [60] P. Sujit, D. Kingston, and R. Beard, "Cooperative forest fire monitoring using multiple UAVs," *IEEE Conference Decision Control*, pp. 4875–4880, 2007.
- [61] F. Su, W. Ren, and H. Jin, "Localization Algorithm Based on Difference Estimation for Wireless Sensor Networks," *International Conference Communication Software Networks*, pp. 499–503, 2009.
- [62] I. Amundson and X. Koutsoukos, "A survey on localization for mobile wireless sensor networks," *MELT, Springer*, pp. 235–254, 2009.
- [63] A. Shaw and K. Mohseni, "A Fluid Dynamic Based Coordination of a Wireless Sensor Network of Unmanned Aerial Vehicles: 3-D Simulation and Wireless Communication Characterization," *IEEE Sensor Journal.*, vol. 11, no. 3, pp. 722–736, 2011.
- [64] D. W. Casbeer, D. B. Kingston, R. W. Beard, and T. W. McLain, "Cooperative Forest Fire Surveillance Using a Team of Small Unmanned Air Vehicles," *International. Journal System Science.*, pp. 1–18, 2005.
- [65] P. Eklund, S. Kirkby, and J. Mann, "A distributed spatial architecture for bush fire simulation," *International. Journal Geographic. Information Science*, vol. 15, no. 4, pp. 363–378, 2001.

References

- [66] T. Tamir, "Radio Wave Propagation Along Mixed Paths," *IEEE Trans. Antennas Propagation.*, vol. 25, no. 4, pp. 471–477, 1977.
- [67] Y. S. Meng, Y. H. Lee, and B. C. Ng, "The Effects of Tropical Weather on Radio-Wave Propagation Over Foliage Channel," *IEEE Trans. Vehicle Technology.*, vol. 58, no. 8, pp. 4023–4030, 2009.
- [68] F. T. Ulaby, M. Whitt, and M. C. Dobson, "Measuring the Propagation Properties of a Forest Canopy Using a Polarimetric Scatterometer ", *Antennas and Propagation, IEEE Transactions on*, vol. 38, no. 2, pp. 251–258, 1990.
- [69] S. Kirkpatrick, C. D. Gelatt, and M. P. Vecchi, "Optimization by simulated annealing," *Science.*, vol. 220, no. 4598, pp. 671–80, 1983.
- [70] T. Tamir, "On radio-wave propagation in forest environments," *IEEE Trans. Antennas Propagation.*, vol. 15, no. 6, pp. 806–817, 1967.
- [71] L. Li, S. Member, and T. Yeo, "Radio Wave Propagation Along Mixed Paths Through a Four-Layered Model of Rain Forest: An Analytic Approach," vol. 46, no. 7, pp. 1098–1111, 1998.
- [72] R. A. Rutenbar, "Simulated annealing algorithms: an overview," *Circuits Devices Magazine. IEEE*, vol. 5, no. 1, pp. 19–26, 1989.
- [73] J. Antonio, G. Fernandez, I. Cuiñas, and M. G. Sánchez, "Radioelectric propagation in a deciduous tree forest at wireless networks frequency bands", *Antenna and propagation (EUCAP)*, pp. 3274–3278, 2011.
- [74] S. Shiodera, T. D. Atikah, I. Apandi, T. Seino, A. Haraguchi, J. S. Rahajoe, and T. S. Kohyama, "Impact of peat-fire disturbance to forest structure and species composition in tropical peat forests in Central Kalimantan, Indonesia," *Boreal Forest Resource.*, vol. 60, pp. 59–62, 2012.
- [75] Y. Ito and H. Igarashi, "Computation of Macroscopic Electromagnetic Properties of Soft Magnetic Composite," *IEEE Trans. Magn.*, vol. 49, no. 5, pp. 1953–1956, 2013.
- [76] V. Pr, R. Corcolle, L. Daniel, and L. Pichon, "Effective Permittivity of Shielding Composite Materials for Microwave Frequencies", *Electromagnetic Compatibility, IEEE Transactions on*, vol. 55, no. 6, pp. 1178–1186, 2013.
- [77] S. S. Tetuko and R. Tateishi, *Tropical Forest Monitoring using Synthetic Aperture Radar*. Chiba University, 2002.
- [78] Q. Wu, N. S. V. Rao, X. Du, S. S. Iyengar, and V. K. Vaishnavi, "On efficient deployment of sensors on planar grid," *Computer Communication.*, vol. 30, no. 14–15, pp. 2721–2734, 2007.

-
- [79] A. Bari, S. Wazed, A. Jaekel, and S. Bandyopadhyay, "A genetic algorithm based approach for energy efficient routing in two-tiered sensor networks," *Ad Hoc Networks*, vol. 7, no. 4, pp. 665–676, 2009.
- [80] B. Krishnamachari and F. Ordonez, "Analysis of Energy-Efficient , Fair Routing in Wireless Sensor Networks through Non-linear Optimization," *Autonomous Networks Resource. Gr.*
- [81] C. Zhao, Z. Yu, and P. Chen, "Optimal Deployment of Nodes Based on Genetic Algorithm in Heterogeneous Sensor Networks," *2007 Int. Conf. Wirel. Commun. Netw. Mob. Comput.*, pp. 2743–2746, 2007.
- [82] F. Herrera, M. Lozano, and J. L. Verdegay, "Tackling Real-Coded Genetic Algorithms: Operators and Tools for Behavioural Analysis," *Artificial Intelligent. Review.*, vol. 12, no. 4, pp. 265–319, 1998.
- [83] <http://www.cgiar-csi.org/data/srtm-90m-digital-elevation-database-v4-1>
- [84] <http://www.memsic.com/wireless-sensor-networks/>
- [85] <http://www.saga-gis.org>

Acknowledgement

First of all, I would like to express my deepest sense of gratitude to my supervisor, Prof. Hajime Igarashi who offered me invaluable opportunity to do my Ph.D thesis under his supervision in Applied Electromagnetic Laboratory, Division of System Sciences and Informatics, Graduate School of Information Sciences and Technology, Hokkaido University; and all of his support, scholastic guided, constructive inspirations, patience and help that enables me to complete this study. I am also thanking to assistant Professor Dr. So Noguchi for all his help and kindness. Moreover I always remember in mind to all my friends in Laboratory of Applied Electromagnetics and very special thanks to Mr. Ryo Murakami and Mr. Yuki Sato for help and useful suggestion. My thanks are due to Ms. Saito, secretary of our Lab, for her assistance and help in official procedure during my study period. I would like to express my gratitude to members of the committee: Prof. Masahiko Onosato, Prof. Hiroyuki Kita for their comment and constructive suggestion and critical analysis on this study.

My deep acknowledgements to Prof. Toshihisa Honma for introduce application of UAV technology in peat forest. Dr. Hidonori Takahashi for introduce behavior of peat fires. All members of CENSUS (Center for Sustainability Science Hokkaido University). Prof. Matsuro Osaki, Prof. Noriyuki Tanaka, Dr Gaku Ishimura. Mr. Yukihiro Shigenaga from Midori Engineering Laboratory Japan.

Many thanks for Prof. Dr. Sulmin Gumiri, Prof. Dr. Salampak Dohong, Dr. Aswin Usop, Dr. Hendrik Segah Patianom, Dr. Fengky Florante Adji for all support and friendship.

I deeply express my special gratitude to the Japanese Government for financial support to conduct my doctor degree through the scholarship program of MONBUKAGAKUSHO. My special thanks to Japanese people for warm welcome in their country, giving their close friendship.

I dedicate this dissertation to my wife. dr. Valencia Wilentine. My parents: Pupu Hermansyah and Rensina Hidik for their ceaseless prayers. Parents-in-law: Tanduk Dilan Hamud (RIP) and Irencé Viktor Nusan for your love. Brother and sister: Benny Pupu, Reny Pupu. Brother-in-law, Jurmandi, Hilman Setiawan Pieter Rogas. Sister-in-law: Yoanitha. All cousin: Elvin Delonio, Englandion Derylio, Benedictus Nathanael Alexander, Theresia Brigitta Nathania.